AD NUMBER
AD459099
CLASSIFICATION CHANGES
TO: **UNCLASSIFIED**
FROM: **SECRET**
LIMITATION CHANGES
TO: **Approved for public release; distribution is unlimited.**
FROM: **Distribution authorized to U.S. Gov't. agencies and their contractors; Administrative/Operational Use; 13 MAR 1953. Other requests shall be referred to Armed Forces Special Weapons Project, PO Box 2610, Washington, DC.**
AUTHORITY
DNA ltr 17 Apr 1973 ; DNA ltr 17 Apr 1973

a/6064

WT-520

Copy No. 227 A

[redacted]

CLASSIFIED

Operation TUMBLER

NEVADA PROVING GROUNDS

April – June, 1952

Project 1.10

PRESSURE-DISTANCE-HEIGHT STUDY OF 250-LB TNT SPHERES

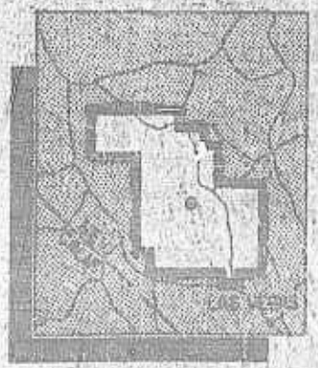

ARMED FORCES SPECIAL WEAPONS PROJECT
WASHINGTON, D.C.

[redacted]

SECURITY INFORMATION

UNCLASSIFIED NO OTS

UNCLASSIFIED

[redacted]

[redacted]

[redacted]

[redacted]

UNCLASSIFIED

(18) AEC

(19) WT-520

This document consists of 107 pages
No. [redacted] of 283 copies, Series A

(21) Report on OPERATION TUMBLER,

Project 1.10.

(6) PRESSURE-DISTANCE-HEIGHT STUDY OF 250-LB TNT SPHERES,

REPORT TO THE TEST DIRECTOR

(10) by
J. D. Shreve, Jr.

March 13, 1953

(5) SANDIA CORPORATION
Albuquerque, New Mexico

[redacted]

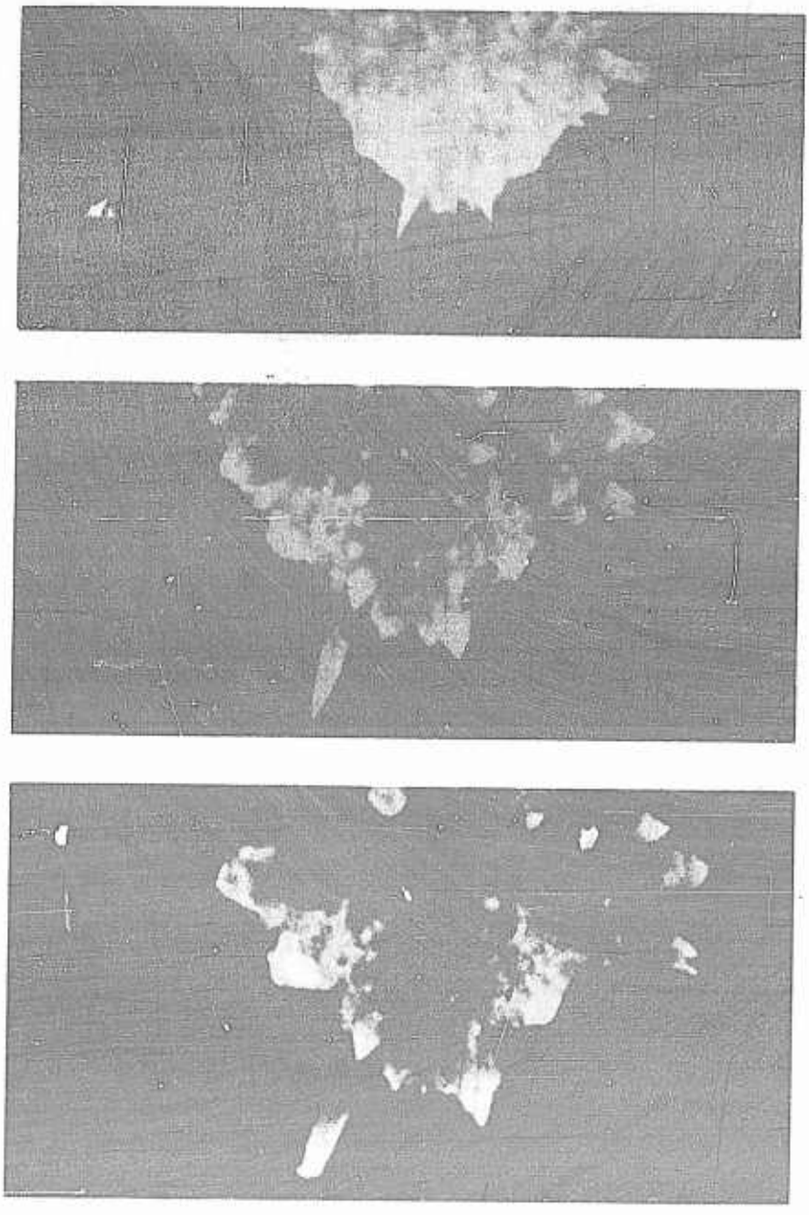

Frontispiece -- High-Speed Sequence of Fireball Growth, (showing lower portion of fireball) on Shot 33, Height of Burst 35 feet. Frames were taken approximately 1.5, 3, and 4.5 msec after detonation. Note progression of large jet, which actually strikes ground in last photograph.

ABSTRACT

An appropriate background against which to evaluate the experimental work reported here is created by a historical survey of the height-of-burst problem which traces the evolution of thinking and the compilation of experimental and theoretical information. The history dates from the initial efforts of the British in their 'model town' study in 1940 to the recent results obtained by AFSWP from the experimental nuclear tests on Operation TUMBLER, and is an effort to integrate the results of experimental and theoretical studies based upon both high-explosive and nuclear bursts.

The ultimate objective of this study was to infer a family of height-of-burst curves from data obtained upon detonation of 250-pound spherical charges of TNT over a smoothed area of the Coyote Canyon test site of Sandia Corporation at reduced heights ranging from zero to approximately 15 ft/lb[illegible]. These curves were corrected to sea level and scaled to 1 pound of TNT and compared with those reported by Hartmann[3] from work with 1-pound pentolite spheres after the latter were expressed in terms of TNT. Areas of disagreement between the two sets of curves are discussed and explanations proffered.

A reflection chart was constructed from experimentally measured reflected overpressures and the Kirkwood-Brinkley free-air curve. The most impressive feature of this chart is the lack of large pressure multiplication in the early Mach reflection region, a result which is contrary to the findings of Porzel-Reines and Pelsor-Prim, who based their treatments on theoretical considerations and shock-tube data.

Finally and perhaps most significant, the applicability of the Sandia and NOL height-of-burst charts to nuclear explosions is evaluated in the light of recent nuclear test data. For surface and near-surface bursts there is a drastic reduction in air blast efficiency for chemical explosives, while only a slight reduction, if any, accompanies similarly situated nuclear explosions according to experience on the JANGLE surface shot. At operational heights in the low to medium range pressure-distance phenomena for nuclear shots are contingent upon effects of intense thermal radiation, which is completely

absent from detonations of high-explosive charges of reasonable size. Even at large operational heights, where thermal levels are comparatively low, pressure-distance data for nuclear shots disagree with those from HE shots. It is concluded, therefore, that an overall solution to the height-of-burst problem by use of data from HE studies is an impossibility. Nevertheless small-scale experiments remain a fruitful field of endeavor, and several specific problems whose resolution might be aided by such investigations are listed for appraisal.

An auxiliary study of the effects of varying the orientation of the side-on baffles used to mount the air gauges was unsuccessful because of the resonance induced in the gauges by vibration of the baffles. Steps taken to eliminate this difficulty are described since they provide meaningful information for future study of the effects of baffle orientation.

Appendix A describes a newly designed 20-kc carrier-amplifier recording system used for the first time on these tests. Appendix B is devoted to an extensive discussion of the Wiancko variable-reluctance gauges used for this study; it contains details of the electrical and mechanical characteristics, damping techniques, and general handling procedures. It also describes an improved model of the gauge which has a shorter bourdon tube of higher mechanical and acoustical frequency. This improved model was used for a large portion of the measurements.

ACKNOWLEDGMENT

This work was sponsored by the Armed Forces Special Weapons Project as Project 1.10 of Operation TUMBLER; Dr. M. L. Merritt of Sandia Corporation acted as project officer.

The field work was ably performed by members of the Field Operations Section, 5112-2, of the Coyote Canyon Division of Sandia Corporation under the leadership of Mr. D. G. Palmer. The 20-kc carrier amplifier recording system used was designed and adapted for field use by Mr. R. O. Ferner, whose authorship of Appendix A describing this equipment is also gratefully acknowledged. The author is indebted to Mr. E. J. Vulgan, both for his work on the adjustment and damping of pressure gauges and his extensive discussion of Wiancko gauges in Appendix B.

Data reduction was done by the Telemetering Section, 5242-2, of the Mathematical Services Division of the Corporation with added assistance by Mrs. Eva Withers and Mr. H. M. Richardson.

Particular credit is due Miss Sally Langenstein for her typing of early drafts, her continual editing of the manuscript, and her execution of the multitude of details attending the preparation of a report for publication.

The author expresses gratitude for the many helpful comments and criticisms of Dr. B. F. Murphey over the course of this study, and for the refinements to the original manuscript suggested by Dr. E. F. Cox.

CONTENTS

ILLUSTRATIONS

ILLUSTRATIONS (cont)

ILLUSTRATIONS (cont)

TABLES

CHAPTER 1

THE HEIGHT-OF-BURST PROBLEM

1.1 HISTORICAL SUMMARY

The possibility of increasing the effectiveness of a weapon (or a charge of high explosive) by bursting it above ground level seems to have had its first experimental demonstration in the work of the Road Research Laboratory.[1] In studying shielding effects this British group burst 2-ounce charges at various heights above a model town and measured peak pressures and positive impulses among the buildings. They attributed the significant increase in damage area observed when the charge was burst at increasing heights to a lessened shielding effect and the fact that energy normally spent, at lower burst heights, in cratering was no longer so diverted.

It was not, however, until von Neumann, in his theory of oblique reflection of shock waves,[2] showed pressure multiplication in the "regular" reflection process to be a nonlinear function of angle of incidence and pressure level that the full import of the British results became evident. Analysis of these earlier results in the light of von Neumann's work spurred the National Defense Research Committee to initiate extensive test programs at the Underwater Explosives Research Laboratory and Princeton University Station: systematic measurements of blast effects from the detonation of 2-, 12.4-, and 42-pound bare TNT charges and 350-, 500-, and 1000-pound bombs at various altitudes provided copious data[3,4] pointing to the increased efficacy of airbursts within a certain range of burst heights. It was found also[5] that when very large charges were burst, positive phase durations exceeded the transit times of the shock over ordinary structures to such an extent that positive impulse gave way to peak pressure as the criterion for predicting damage.

It was these meaningful disclosures, authenticated by cogent experimental evidence, that led to the basic conclusions (1) that the detonation of a charge of given weight at any specific burst height maximized the horizontal ground distance to some overpressure level and (2) that choice of an appropriate burst height hinged upon the pressure

level thought necessary to destroy the target.

Thus in the years between 1941 and 1944 the full implication of height of burst as a major contributory factor in the effectiveness of chemical explosions had become fundamental knowledge, as had the scaling laws relating pressure-distance curves from detonation of charges of different weights. In March of 1945 the National Defense Research Committee held a symposium on airburst for blast bombs[6] in which the experimental basis for airburst and some specific effects of burst position on target destruction were treated. Apparently the military significance of airbursts had been realized for some time, for this symposium included a talk on variable time fuzing for airburst bombs. Other presentations indicated that the theory of regular reflection was well established, and a comprehensive study at the Underwater Explosives Research Laboratory[4] of pressures in the Mach region had led to a good empirical description of triple-point loci and Mach stem pressures. It is not difficult to perceive the tremendous implications of this symposium, preceding as it did the historically indelible dates of August 6 and August 9 of the same year.

It was not until two years later, in August 1947, however, that the procedure used in extending height-of-burst data from high-explosive detonations to the scale of nuclear explosions was treated in a publication.[7] Reines and von Neumann surveyed existing experimental data on airbursts of nuclear and high-explosive charges, reviewed the status of theoretical and empirical descriptions of reflection phenomena, initiated the present-day form of the height-of-burst chart, and extrapolated pressure-distance and Mach stem information to the realm of the nuclear weapon. Unfortunately their calculations and specific recommendations were based upon data[3,4] which were later vitiated because of incognizance of the effects of charge shape and the use of inadequate pressure-sensing instruments and techniques.

For it was at about this time that Stoner and Bleakney[8] were to report the results of their measurements of pressure-distance relations for detonation of TNT blocks and cylinders and pentolite cylinders and spheres which demonstrated incontestably the influence of charge shape upon the pressure pattern; realizing, too, the inadequacies of existing pressure-sensing devices, these authors were the first to employ measured shock velocities to reckon overpressures by means of the Rankine-Hugoniot relations.

Another contribution of this work by Stoner and Bleakney was to corroborate* the theoretical blast-wave curve of Kirkwood and Brinkley[9] for TNT. Although Kirkwood and Brinkley had published their results in 1945, reference to their work was conspicuously omitted from subsequent reports until its mention by Stoner and Bleakney. Actually the discrepancy between the theoretical results for TNT and experimental data from TNT detonations was not explicable until the magnitude of the effect of charge shape was brought to light.

Meanwhile the initial experimental airburst of a nuclear weapon during Operation CROSSROADS had taken place at the Pacific Proving Grounds and had provided the first experimental pressure-distance data[10] for a nuclear explosion. Porzel and Reines,[11] working somewhat intuitively, had constructed an overpressure reflection chart for the full gamut of angles ranging from normal to grazing incidence,† based upon von Neumann's theory of regular reflection,[2] Taub's small-charge data,[5] and the assumption of 1.5 as the free-air equivalent charge weight ratio at large distances (angle of incidence approaching 90^{o}). This reflection chart could then be used with the measured reflected overpressure‡ as a function of distance for a nuclear explosion to infer a free air pressure curve for Bikini Shot Able. By comparing this curve with the Stoner-Bleakney curve for pentolite spheres, Porzel and Reines computed the average blast efficiency§ of Shot Able to be 0.75 for the overpressure range of 4 to 20 psi. Finally they combined the free air pressure data from pentolite spheres with their

*Taking the differences in energy release for pentolite and TNT into account.

†This approach to the problem had previously been outlined by von Neumann and Reines (loc. cit.); the work of Porzel and Reines was intended to supercede this particular chapter of the earlier publication.

‡Original Bikini results were re-examined and evaluated anew in the Scientific Director's report on Operation SANDSTONE,[10] and these later values were employed by Porzel and Reines.

§Blast efficiency is simply the fraction, f, of the radiochemical yield, W_{RC}, of a nuclear explosion going into blast. It is arrived at in the following manner. Choose a pressure level (cont on next page)

$$\frac{W_B}{W_{TNT}} = \left(\frac{R_B}{R_{TNT}}\right)^3 \qquad f = \frac{W_B}{W_{RC}}$$

R_B = Range for a given pressure level from a nuclear explosion.

reflection chart data (varying the burst height appropriately) and scaled the resultant reflected overpressure-distance information to unit radiochemical yield (1 KT), using the blast efficiency factor and conventional cube root scaling. This procedure gave a complete family of height-of-burst (p-d-h) curves for nuclear explosions. But the authors, aware of undesirable uncertainties in their assumptions and in the accuracy of the small-charge data used, emphasized the need for direct measurement of free air pressures for nuclear explosions and made the following statement concerning related experimental measurements from high-explosive detonations: "It is suggested that experiments designed to measure the reflection pattern be conducted using larger ($\simeq$500 pounds) H.E. charges....to facilitate measurement of the Mach pattern and minimize the effect of surface irregularities. Charges should be spherical in shape and detonated at the center."

In July of 1950 this work of Porzel and Reines was challenged by Pelsor, who claimed[12] that the reflection chart used for their study stemmed from questionable assumptions. Reasoning from the shock-tube results of Smith[13] he asserted that a much more pronounced pressure multiplication accompanied the onset of Mach reflection. In addition, he proposed that a reflection factor (free air equivalent charge weight ratio) of 2.0 was more realistic than 1.5 for a large-scale explosion, and constructed a new reflection chart incorporating the altered assumptions and ignoring the small-charge data of Taub. Next he evaluated the blast efficiency in the established manner except that he arbitrarily confined his comparison of data from pentolite and nuclear explosions to three reflected overpressures (11.1, 16.5, and 22.7 psi) as indicated by shock-velocity measurements on Bikini Shot Able.*

---

and read the corresponding distance from each of the free air pressure-distance curves, that for the nuclear explosion and that for TNT. The cube of the ratio of the two distances read equals the ratio of the blast yields of the two explosions considered. Knowledge of the TNT yield then allows determination of the blast yield, W_B, of the nuclear explosion. The quantity W_B divided by the total or radiochemical yield, W_{RC}, gives the blast efficiency, $(W_B/W_{RC}) = f$. The 0.75 computed by Porzel and Reines on the basis of pentolite must be corrected prior to comparison with blast efficiencies based on TNT. This is made clear later in this report.

*As did Porzel and Reines; Pelsor used data as given in the Scientific Director's report on Operation SANDSTONE. [illegible] appears that Pelsor used original Bikini data from the [illegible] (Operation Crossroads) [illegible] (XRD-212)

He arrived at a blast efficiency of 0.46 as contrasted with that of 0.75 computed by Porzel and Reines. Still using the method followed by them, he constructed a new height-of-burst chart; as would have been anticipated, these curves exhibited marked disagreement with their predecessors. Actually, however, the discrepancy is not entirely accounted for on the basis of the change in assumptions; a good share of it is attributable to the use of differing values for reflected overpressure:

Radial distance (ft)	Reflected overpressure (psi) (Pelsor - SC-1516(TR))	Reflected overpressure (psi) (Porzel and Reines - LA-743R)
2,454	16.5	18.4
3,040	11.1	12.0

A controversial period ensued. An endeavor to resolve this controversy was made in publishing the Bode-MacNair report[14] in May 1951 in which Pelsor collaborated with Prim in a reassessment of the problem. The outcome was essentially a more elegant statement of Pelsor's earlier analysis with one added refinement: the relative effectiveness of pentolite and TNT were recognized. Prior to this time the blast efficiency had been determined by direct comparison of data from nuclear explosions with the pentolite data of the Stoner-Bleakney article[8] despite the traditional expression of radiochemical yield in kilotons of TNT and despite the establishment of the inequality of pentolite and TNT* in the same artic'e. Pelsor and Prim accordingly took 1.18 pounds of TNT as the equivalent of 1 pound of pentolite, reused Pelsor's earlier reflection chart, but used data from Bikini Shot Able as given in LA-743R to arrive at a blast efficiency of 0.63 for a nuclear explosion in air.† It must be understood that for comparison with the earlier blast efficiences of 0.75 and 0.46 this revised value for blast efficiency must be stated in terms of the pentolite equivalent, 0.63/1.18 or 0.53; this is the blast efficiency that Pelsor would have arrived at had he chosen to use the same values for reflected overpressure as were used by Porzel and Reines in their earlier computations. This reappraisal culminated in the construction of still another family of height-of-burst

*By admission of the validity of the Kirkwood-Brinkley theoretical curve for TNT spheres.

†Fireball at no time in contact with the reflecting surface.

curves, ambiguously termed the P^2 curves (the result of a multiplicative process involving the final initials of their authors); apparently a good deal of confidence accompanied these results.

In one respect it was extremely fortunate that Bikini Shot Able, upon which these early height-of-burst curves were based, was detonated over water. The reflection phenomena observed on this burst were probably the simplest possible, giving a pressure-distance relation as nearly ideal as could be expected from a burst at this low height. The fortuitous choice of conditions in all likelihood accounted not only for the smoothness of the pressure-distance data but their excellent correlation, upon scaling, with existing small-charge data. The ideal nature of the results is seen in the blast efficiencies calculated by the several investigators cited above. Each found the quantity to be surprisingly insensitive to pressure level selected (ranging from about 4 to 20 psi). An unfortunate consequence of these ideal test results was the implication that they described typical results of nuclear explosions.

How atypical this behavior was did not become recognized for some time. In fact, it was not until Operations GREENHOUSE, BUSTER-JANGLE, and TUMBLE-SNAPPER had been executed and the results assayed that anything approaching general agreement was reached concerning the complex interplay of effects from a "Bikini Able" over land.

Pressure-distance-time data obtained on Operation SANDSTONE[15] had been the first to evince an inexplicable attenuation of peak overpressures. A degeneration of the shock front into a slowly rising pressure-time profile was also found to be prevalent at pressure levels of interest. At that time the data were held in abeyance, their peculiarities deemed the result of inaccuracies of the instrumentation.

Operation GREENHOUSE,[16] which consisted entirely of tower shots, afforded a good check of the SANDSTONE anomalies. Since exceptional care was taken with instrumentation, the GREENHOUSE results carried a high confidence factor. When these results corroborated those of SANDSTONE, their peculiarities were accepted as behavior to be expected from tower shots over land.

The results of Operation BUSTER[17] merely served to reinstate the earlier confusion; the pressure-time records from airburst Shots Charlie and Easy were so misshapen and distorted that they had little

resemblance to a normal blast wave profile. There was no course open but to take the maximum pressures indicated by the gauges as the peak pressures even though they were attained as late as the middle of the positive phase. When the peak pressures thus obtained were plotted on existing height-of-burst charts, not only were the deviations from predicted results marked, but there was considerable disagreement between the results of Shots Charlie and Easy. Since these two shots had been detonated at virtually the same scaled height and over the same type of terrain, it was concluded that the height-of-burst curve should be pictured as a broad band rather than a line. Many investigators still held to the opinion formulated after Operation SANDSTONE -- suspect instrumentation. Others,[18] assuming the validity of the BUSTER results, constructed multiple isobars for the same pressure, labeling the bounded regions as poor, fair, and good. The actual conditions that caused results to fall within one of the regions so defined remained a matter of educated guesswork. The results of Operations SANDSTONE, GREENHOUSE, and BUSTER combined, however, to give credence to the possibility that the decreases in pressure level and the distortions of the shock wave were manifestations of previously unexplored phenomena. For instance, it was suggested that the low pressures observed might be an indirect result of the heating of the layer of air near the ground by thermal radiation from the fireball or of the dissipation of energy in raising the huge clouds of dust and overcoming the resultant turbulence. Satisfactory experimental corroboration or refutation of these qualitative explanations had to await completion of the TUMBLER series of nuclear airbursts, however.

Operation TUMBLER provided pressure-distance-time data[19, 20, 22] on airbursts of four weapons detonated at three* distinctly different scaled heights. The lowest of these, Shot 4, was at a scaled height of approximately 560 feet, and the resultant data were characterized by the same peculiarities noted earlier on BUSTER Shots Charlie and Easy and on GREENHOUSE Shots Dog and Easy. The claim of faulty instrumentation on prior operations was invalidated in the face of the essential agreement of direct pressure measurements made independently by four separate agencies using three different types of pressure-sensing elements. Thus the results of TUMBLER Shot 4 confirmed the hypothesis that low bursts could give clean pressure waveforms and 'ideal' pressure-distance relations only under very special conditions indeed -- say those of Bikini Able. A valuable clue to the anomalous behavior of a blast wave

*Shots 2 and 3 were scaled to practically the same height.

over a land reflector came with the photographic detection of a separate shock wave running in advance of the incident shock front, and reexamination of several of the pressure-time records brought to light clear evidence of separate compression waves together with their relative magnitudes and their sequence in time. In fact, there was sufficient evidence to permit a first approximation of conditions required for the formation of such a forerunner or precursor.[22] Furthermore, estimates of its attenuation and duration have been made. The significant point to be made here is that the complexity of the mechanism for precursor formation and propagation is such that a cloak of uncertainty is cast upon pressure-distance predictions. The authors of the preliminary report on Operation TUMBLER,[20] being well aware of this situation, presented two height-of-burst charts. In one the isobars were delineated by use of experimental data from Operation TUMBLER alone* except for the zero-height intercepts, which were the results of the JANGLE surface shot.[21] The other chart presented pertinent isobars from the first and correlated data from all successfully instrumented nuclear airbursts. A shaded area enclosing all data for a given pressure level was drawn to represent the extent of scatter that might result from conceivable extremes in reflecting surfaces. The current status of the height-of-burst problem is just about as described in this TUMBLER report.

1.2 SCOPE OF CURRENT STUDY

The degree to which experimental studies using chemical explosives can assist in resolving certain phases of the height-of-burst problem is the principal consideration of this report. In the period following Operation BUSTER confidence in existing height-of-burst curves was at low ebb. Because the predictability of pressure-distance relations was in question, plans for Operation TUMBLER included a preliminary study (Project 1.10) intended solely to obtain pressure-distance-time data from scaled bursts of nominal 250-pound spherical charges of TNT. It was planned that data from these bursts, over the areas at the Nevada Proving Grounds to be used for TUMBLER Shots 1-4, would not only permit more accurate prediction of overpressures for the forthcoming TUMBLER shots but would provide useful comparative

*In regions above the experimental points the curves were inferred from reflection theory and the measured free-air curve for Operation TUMBLER.

information for interpreting results obtained on earlier nuclear tests. The fact that little thermal radiation accompanies a small TNT explosion would, it was believed, make it possible to establish whether the observed reduction in overpressure was a function of mechanical effects alone. A further refinement of the evidence was thought possible because the two areas at Nevada Proving Grounds over which the charges were to be burst differed fundamentally in superficial terrain characteristics: that at Area T-7 was light tan in color and had a shallow layer of loosely packed gravelly sand covering a hard subsurface layer, whereas that at Frenchman Flat was almost white and had a hard-packed clayey surface (time: early spring) which was not so prone to disturbance. Thus if mechanical effects played a significant role in decreasing overpressures, it seemed probable that these preliminary TNT shots would provide evidence of these effects.

Two sets of three shots each were originally scheduled under Project 1.10; they were to be fired at scaled heights of 47, 37, and 22 feet over the areas designated. The burst heights of 47 and 22 feet were scaled from the intended burst heights for TUMBLER Shots 1 and 4; that of 37 feet corresponded to no planned or past shot* but served as an intermediate set of conditions. When it became evident that a preliminary check-out of the test instrumentation as well as some clue as to the reproducibility of results were desirable, an additional six shots were scheduled at the Coyote Canyon test site,† making a total of 12 in all. Since these shots at Coyote Canyon were to be burst over still another type of reflecting surface, it was realized that the range of comparison for the mechanical effects under investigation could be still further extended. Thus Shots 1 and 2 were burst at Coyote Canyon, Shots 3-5, over Area T-7, Shots 6-8 over Frenchman Flat, and the remaining four at Coyote Canyon.

Upon completion of these pre-TUMBLER measurements it was pointed out to AFSWP,‡ at whose request the original tests were run, that the Sandia Laboratory was contemplating an exhaustive height-of-burst study using 250-pound TNT spheres. It was thereupon agreed

---

*Possible exception is the burst over Nagasaki.

†The high-explosives blast site of Sandia Corporation, supported largely by AFSWP.

‡Armed Forces Special Weapons Project

that AFSWP would sponsor the study as an extension of Project 1.10, and an additional series of 48 shots was scheduled to be carried out at Coyote Canyon in the late fall and winter of 1952.

Some modification of the original test setup, as it had been described in a preliminary report[23] on the initial series, was necessary for the height-of-burst measurements. The blast line was lengthened to permit pressure measurements at greater distances from ground zero. To better the time-resolution of the measurements the gauge and recording systems were completely revised, as described in Appendixes A and B. Since the projected height-of-burst study naturally encompassed the observation of free air overpressures and such phenomena as Mach stem formation and attendant variations in pressure at increasing heights above ground level, it was necessary to install air measuring stations at strategic levels above the ground at several positions along the line of ground stations. But perhaps most important was the provision to burst the charges at greater and lesser scaled heights than on the initial series as well as at ground level. As further amplification of the measurements of air pressures above ground level it seemed propitious, as an integral part of the height-of-burst study, to conduct a controlled experimental investigation of such related problems as the efficacy of various types of air baffle and optimum baffle orientation.

CHAPTER 2

INSTRUMENTATION

2.1 THE BLAST LINE

A complete description of the instrumentation for the blast line used on the pre-TUMBLER measurements has already been published[23] and will be mentioned only briefly here. It had a maximum extent of 200 feet and consisted of flush ground gauges on a single radial line at distances of 0, 12.5, 25, 37.5, 50, 62.5, 75, 87.5, 100, 125, 150, and 200 feet from ground zero. For the height-of-burst study the blast line was lengthened to 275 feet (Fig. 2.1) and comprised 18 ground-level stations plus 12 pipe stations for mounting the air baffle gauges. The ground stations were appropriately spaced on a single radial line leading outward and on a slight upward slope (Table 2.1) from ground zero, and the pipe stations were on a line parallel to and 5 feet from the line of ground stations.

For ground-level measurements the end instruments were mounted flush with the surface of the ground in recessed 18-inch segments of 3-inch ID galvanized water pipe (Fig. 2.2); for measurements at various elevations above ground level the gauges, in side-on baffles, were mounted at the outer extremities of 30-inch side arms on pipe stands 20 feet high (Figs. 2.1 (inset) and 2.3). Ten of these pipe stands were available, six of which had side arms at the 1.5- and 20-foot levels only. This limitation had to be taken into account in planning gauge arrays for individual shots. The mounts for the baffles were so designed that the baffles, to which the gauges were attached, could be properly oriented with respect to ground zero or the charge position.

Since the capacity of the recording system limited the number of channels of intelligence recorded on any single shot to 18, the gauge array was necessarily restricted to a maximum of 18 locations. The blast-line configurations for all shots, in terms of station designations indicated in Fig. 2.1, are presented in Table 2.2 with other pertinent information such as height of burst, baffle orientation, and measured ambient conditions. The intended total of 48 additional shots was

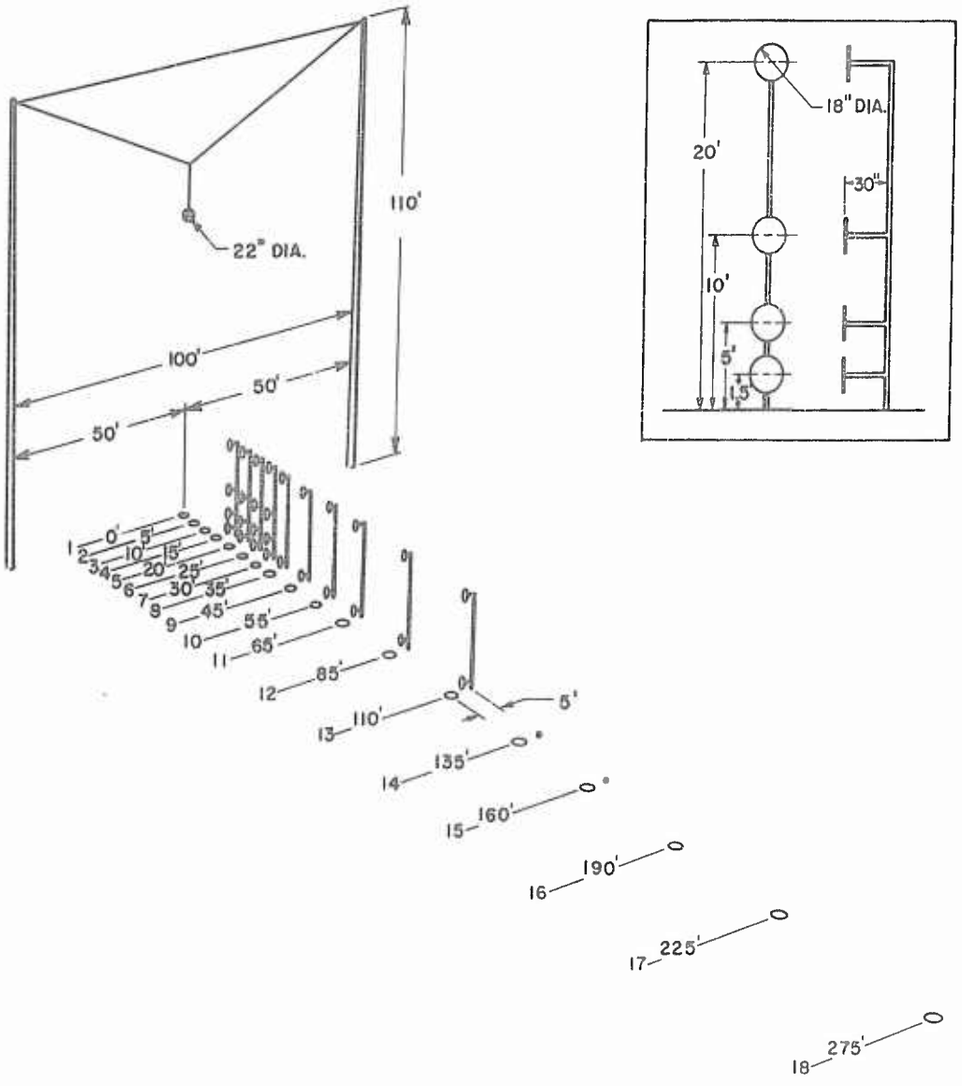

Fig. 2.1 -- Layout of Blast Line and Charge Suspension System

TABLE 2.1

Survey of Blast Line Stations

Station No.	Distance (ft)	Elevation above ground zero (ft)
1	0	0
2	4.95	0.030
3	9.95	0.065
4	14.98	0.095
5	19.98	0.135
6	24.87	0.220
7	29.94	0.290
8	34.91	0.335
9	44.89	0.430
10	54.91	0.590
11	64.83	0.765
12	84.95	1.235
13	110.00	1.835
14	134.82	2.380
15	159.84	2.765
16	190.00	3.380
17	225.10	3.840
18	275.05	5.280

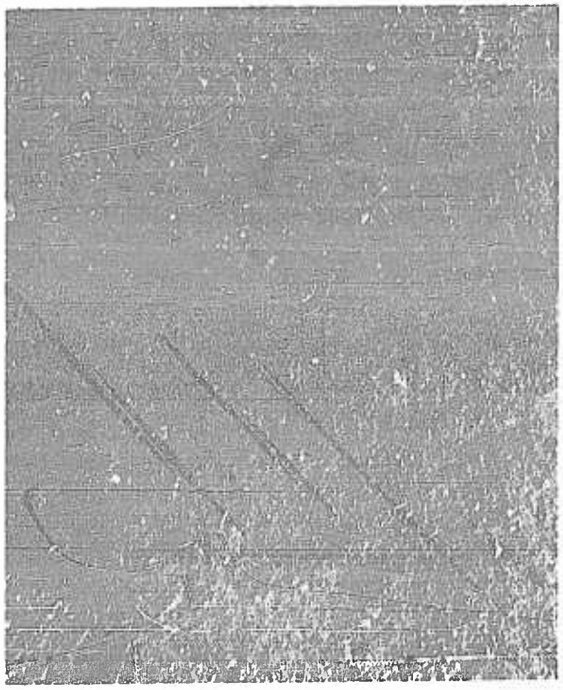

Fig. 2.2 -- Wiancko Gauge Mounted for Ground-level Pressure Measurements

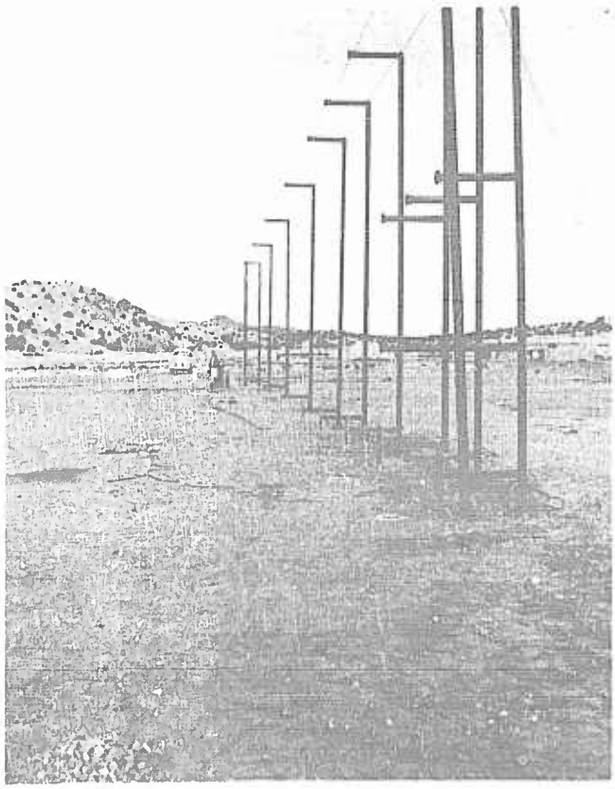

Fig. 2.3 -- View of Blast Line from Ground Zero, Showing Pipe Stations. Note gauges in square baffles at 1.5-foot level.

revised to 34 because of the pressure of other programs scheduled at the test site. In some instances tests were repeated one or two times to obtain information on the degree of scatter to be anticipated in the data, i.e., the extent to which results were reproducible.

Ground-level measurements only were made on Shots 13-19 at burst heights ranging from 70 to 100 feet. On Shots 20-30, at burst heights ranging from one to 70 feet, two ground stations were replaced by air-baffle stations at the 20-foot level so that simultaneous reference measurements of free air overpressure could be made.

Shots 39, 40, and 41, all at a height of 35 feet, were designed specifically to make free air overpressure measurements. These measurements were made at the 20-foot level at eight different stations (Fig. 3.5).

Although the primary objective of Shots 31-38 was to measure variations of incident and reflected overpressure with distance and height above ground, it was found that, within the limitations imposed by availability of pipe stations and predetermined gauge heights, several pairs or groups of three gauge positions were equidistant from the charge at certain of the planned burst heights. This chance circumstance prompted a parallel investigation -- a study of the effect of baffle orientation on pressures seen by the gauges.

Shots 42-46 were intended specifically to compare pressures at ground level with those measured at the 1.5-foot level for both high and low burst heights.

Power cables from the 20-kc carrier system to the gauges and return leads to the recording system were carried underground to gauge stations 50 feet or less from ground zero through a series of interconnecting trenches. At farther-out stations the cables were run along the ground surface.

To minimize any attenuating effect on the shock wave that might be exerted by surface dust the blast line area was carefully watered prior to each shot. Since the same ground zero was used for all shots, craters formed by surface and near-surface bursts had to be backfilled and the fill compacted as thoroughly as possible before another shot was fired.

TABLE 2.2

Operations Log

Date	Shot No.	Height of burst (ft)	Charge weight (lbs)	Ground stations*	Air stations*	Barometric pressure (mm of Hg)	Relative Humidity (%)	Temp. (°F)	Wind velocity (estd) (mph)
2/4/52	1‡	47	-	9 stations at 12-1/2' intervals, plus 2 at 25' intervals, and a final station at 200'	None	-	-	-	-
2/4/52	2	37	-		None	-	-	-	-
2/13/52	3	47	249.5		None	25.96	-	39	10-13
2/14/52	4	37	252.5		None	25.90	-	38	15-20
2/14/52	5	22	251.5		None	25.91	-	42	15-20
2/16/52	6	47	249.5		None	-	-	56	15-20
2/17/52	7	37	253		None	-	-	48	35
2/17/52	8	22	251.75		None	-	-	45	40
2/27/52	9	47	250.75		None	24.15	20	52	5
2/28/52	10	37	-		None	24.97	-	56	20
2/29/52	11	37	-		None	24.00	18	61	5
3/4/52	12	22	-		None	24.00	40	41	35
9/24/52	13	80	250	1-18	None	24.25	26	79	8
10/1/52	14	80	-	1-18	None	24.20	26	78	5
	15	70	254.5	1-18	None	24.15	18	81	4
10/2/52	16	90	255.5	1-18	None	24.35	26	75	8
	17	100±1	256.5	1-18	None		----Low-order---- detonation		
10/3/52	18	100	-	1-18	None		-- Log sheet missing--		
	19	70	-	1-18	None		----Low-order---- detonation		
10/6/52	20	60	255	1, 3, 4, 6-18	9D, 13D	24.15	16	79	6
10/9/52	21	50	251.6	1, 3, 4, 6-18	9D, 13D	24.15	17	81	1
10/11/52	22	45	256	1, 3, 4, 6-18	9D, 13D	24.25	14	80	4
10/13/52	23	40	256	1, 3, 4, 6-18	9D, 13D	24.08	13	76	10
10/14/52	24	35	253.5	1, 3, 4, 6-18	9D, 13D	24.1	7	71	1
10/24/52	25	30	254	1, 3, 4, 6-18	9D, 13D	24.05	24	74	5
10/18/52	26	25	256	1, 3, 4, 6-18	9D, 13D	24.30	13	71	2.5
10/21/52	27	20	256.5	1, 3, 4, 6-18	9D, 13D	24.25	20	66	6
10/22/52	28	15	257	1, 3, 4, 6-18	9D, 13D	24.23	19	72	10
10/23/52	29	1	253.5	1, 3, 4, 6-18	9D, 13D	24.25	21	74	12
10/27/52	30	1	254.5	1, 3, 4, 6-18	9D, 13D		19	76	5
11/22/52	31	15	254.25	5-16	8C, 8D (+12°)				
12/11/52	31R		259		9C, 9D (0°) 10C, 10D	24.30	45	51	0-5
12/13/52	32	35	258.75	1, 4, 6, 8-15, 17, 18	6B, 7C 10A, 11A&C	24.30	36	52	5
12/15/52	33	35	262.5	1, 3, 5, 7-15, 17, 18	4B, 6B 7C&D	24.25	42	54	-

TABLE 2.2 (cont)

Date	Shot No.	Height of burst (ft)	Charge weight (lbs)	Ground stations*	Air stations*†	Barometric pressure (mm of Hg)	Relative Humidity (%)	Temp. (°F)	Wind velocity (estd) (mph)
12/16/52	34	40	258.25	1, 3, 5, 7, 9, 15, 17	5B&C 7A, 7D(0°), 8C(-4°), 8D(-15°)	24.10	24	50	0-5
12/17/52	35	40	254.75	1, 3, 5, 7, 9, 15, 17	5B&C 7B, 7D(+12°) 8C(-10°), 8D(0°)	24.05	42	53	5
12/19/52	36	45	257.75	1, 3, 6, 8-15	4B(+15°) 6C, 8D(-15°) 9B, 10D, 11A&12A	24.20	50	50	4
12/20/52	37	50	259.5	1, 4, 6, 8-18	4B(-5°), 6C 7B(-8°), 9D	24.10	50	44	-
12/23/52	38	55	258.75	1, 4, 6, 8-10 12-16	5B&C 7C(-3°), 8C(-5°) 8D(-7°), 9D	23.95	76	42	4
12/29/52	39 40 41	35	258.25 257.75 259.25	1, 4, 7, 9, 10 15, 17, 18	6-15D	24.10	54	39	-
12/31/52	42 43	80 70	259 257	6, 8-15	6A, 8-15A(0°)	23.95	65	44	-
1/2/53	44 45 46	5 2 0(half buried)	259.25 259.5 256	6, 8-15, 17	8-15A(0°)	24.45	68	41	5

*Station Nos. are shown in Fig. 1.1; †Numbers in parentheses specify baffle orientation designations; standard orientation of +6° not specified; ‡Preliminary shots 1-12, as discussed in Sandia Corporation Memorandum report 5111(65) by B. E. Murphey, comprised 6 shots at Nevada Proving Grounds and 6 shots under similar circumstances at the Coyote Canyon test site.

2.2 THE GAUGE AND RECORDING SYSTEM

Variable-reluctance bourdon type air pressure gauges* manufactured by the Wiancko Engineering Company were selected as end instruments for this study. At the time of the pre-TUMBLER measurements the Wiancko 3PAD gauge was the only one of this type available in sufficient quantity to instrument these tests. Actually the 3PAD gauge was more than adequate in response characteristics for the recording system with which it was used in Nevada since little in excess of 1000-cps information could be recorded using that system. At the start of Operation TUMBLER, however, work had begun on a 20-kc carrier system designed to record 3000-cps information, and 3PAD gauges of the lower pressure ranges did not have a high enough frequency response for use with this system. Therefore, upon request, the manufacturer modified the gauge to increase its frequency response and lessened the coil inductances to make them more compatible with the 20-kc carrier. Use was made of this modified gauge (Mod 20PAD-WS) whenever possible on the extended height-of-burst study. Unfortunately too few were available at the time to permit their exclusive use.

Each gauge was checked in the laboratory for mechanical and acoustical damping (App B) prior to use in the field. While acoustical damping was made as complete as possible, mechanical damping was adjusted to give a damped wave train of 3-4 cycles.† An oscillogram of the output of each gauge in response to a shock wave was made as a permanent record of its response characteristics. Between Shots 31 and 32 all gauges were cleaned and redamped to offset the possibility of inhibition of response by accumulated dust and moisture. For while every precaution was taken during intervals between shots to prevent

*Detailed descriptions of the design, operation, and laboratory calibration of the recording and gauge systems are presented in Appendixes A and B to this report.

†Underdamping to this extent allows for an increase in damping force concomitant with lower temperatures. In the opinion of the author a pressure-time record incorporating some evidence of gauge 'ring' is more easily interpreted than one from an overdamped gauge.

dust or moisture from entering the bourdon tubes of the gauges, no protective measure is possible against the dust raised by the explosion or the moisture of condensation.

Checkout and initial application of the pressure-recording system indicated a normal and inherent tendency for drift with changing ambient conditions. In addition, the gauges undergo slight changes in response characteristics upon continued use in the field. Because the constantly changing configuration of the blast line made it impracticable to reuse identical combinations of gauge, amplifier, galvanometer, and cable, it was necessary, immediately prior to each shot, to perform static calibrations of the individual gauges in combination with their assigned amplifiers, galvanometers, and cables. A static pressure equivalent to the predicted pressure at the particular gauge station was applied at the gauge, using a Grove regulator and a Heise bourdon gauge. This recorded calibration signal later served as a standard for reading the actual experimental pressure-time record from the gauge.

Since one to three hours was consumed in calibrating the 18 gauges and readying the charge for detonation, provision was made for a check of the electrical systems on all channels immediately before and after the shot. As each gauge was calibrated statically a resistor-capacitor combination was chosen which closely matched the output of the gauge at the calibration pressure. This simulated signal was recorded also. These calibration units were connected through relays, each unit to its proper channel, and the entire bank of units was actuated from -1 to -0.5 second and again from +3 to +3.5 seconds by the program timer, which also fixed the sequence of other events such as actuating equipment voltages, starting cameras, and initiating the detonation. Thus calibration steps were recorded on the film immediately before and after the pressure-time recording and served as the amplitude standard for each channel as well as a dynamic check upon the electrical system. This last feature is important in that the receiver-galvanometer combination has adjustable damping also.

Sources of error in measurement, introduced by factors external to the gauge, were carefully explored. The Heise bourdon gauges* used for static calibration had a guaranteed accuracy of 0.5 per cent of full scale pressures greater than 20 per cent of nominal range and

*Gauges having nominal ranges of 15, 30, 60, 100, 200, and 500 psig were used.

0.2 per cent at pressures less than 20 per cent of nominal range. When compared with a dead weight standard these gauges were found to be well within the manufacturer's specifications. Their reading accuracy was commensurate; the smallest scale division was a maximum of 1/300 full range, and interpolation to half divisions was easily possible.

The time base for the oscillograph film was a 2-kc sine wave supplied by a timing unit built by American Time Products, Inc. It had a rated precision of 1 part in 100,000 and a temperature coefficient of 1 cycle per 10^6 cycles per degree centigrade in the range of 0^o to 70^oC. Checks against WWV indicated a maximum deviation of 1 cycle in 13 seconds or 1 part in 26,000 (better than 0.04 per cent). Back-up timing of 1 per cent accuracy was built into the oscillograph (App A).

2.3 AIR BAFFLES -- CONFIGURATION, DAMPING, ORIENTATION

It has been recognized for some time that perturbation of air flow by blast gauges is a definite deterrent to accurate pressure measurement, and a number of expedients have been tried for streamlining high-velocity flow across sensing elements in free air. Theoretical calculations and experiments,[24,25] both in shock tubes and in the presence of actual blast waves, have considered a variety of streamlined bodies as gauge mounts, and estimates of flow perturbations in terms of errors in measured pressure were made. It is on the basis of these studies that a 17- or 18-inch square or circular baffle of half-inch metal plate has come into common usage[19,26,27] with Wiancko variable-reluctance gauges. Figures 2.4, 2.5, and 2.6 show the usual flush mounting of the gauge in the baffle; the side-arm type stand-off is more or less standard for isolating the baffle aerodynamically from the vertical post.

Any quantitative assertions concerning the effectiveness of this single-faced baffle must, however, be held in question, for all published material found to date has treated symmetric or double-faced configurations. The first specific experimentation with single-faced baffles to be reported appears to have been the wind-tunnel tests by Sandia Corporation of an 18-inch circular baffle of 1/2-inch aluminum plate.[28] The effect of yaw was determined as a function of

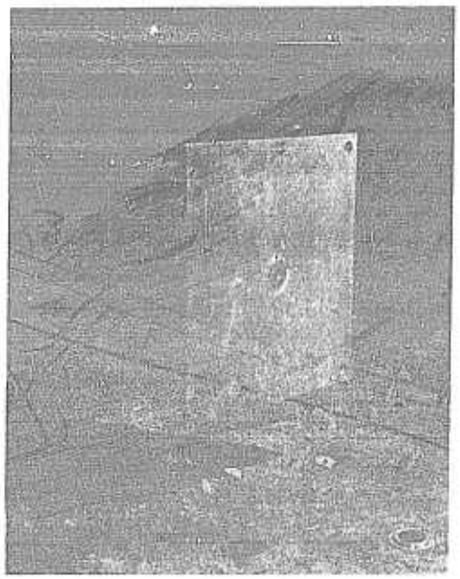

Fig. 2.4 (left). -- Square Baffle with Butt Edge, in Place on Pipe Stand. Note pipe cap and chamfered retaining ring for ground gauge in foreground.

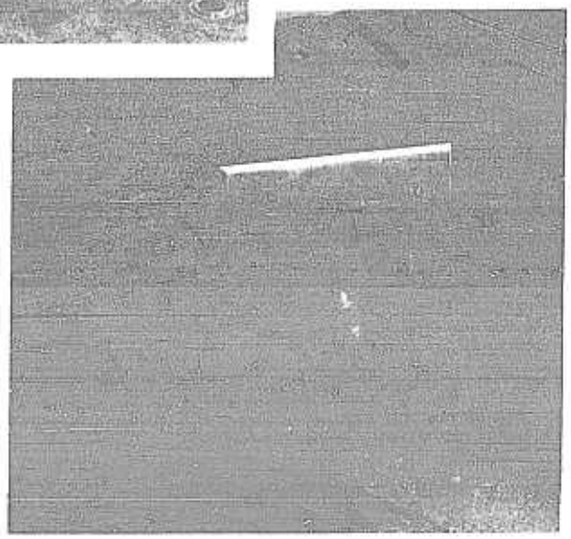

Fig. 2.5 (above). -- Square Baffle, Beveled Edges

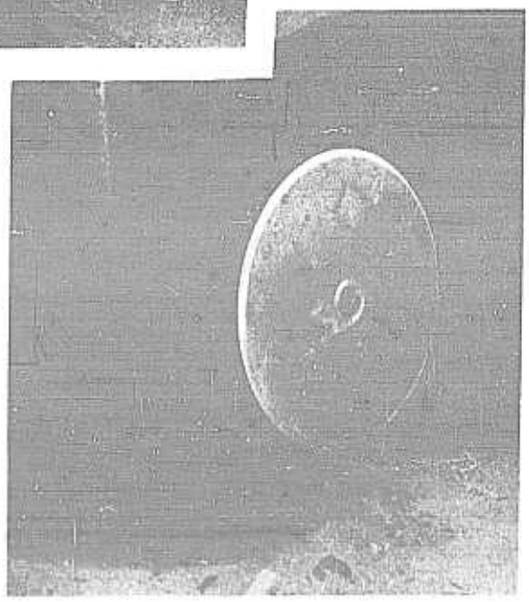

Fig. 2.6 (right). -- Circular Baffle, Beveled Edge

anticipated peak material velocities and densities for blast-wave overpressures in the range of 3 to 13 psi. Here again acceptance of the data must be conditional, for the results are indicative only of steady-state behavior in the absence of a shock wave. A cursory field check of the wind-tunnel test results by Stanford Research Institute on Operation TUMBLER[27] showed that improper baffle orientation caused errors in measured overpressures of the sign predicted by the wind-tunnel tests and that the error for a given orientation angle increased with overpressure. Although the quantitative correlation was not good, in view of the limited number of measurements made, the small overpressure range investigated, and the lesser precision of field measurements as compared with those in the wind tunnel (probably less by an order of magnitude), one cannot conclude that field and wind-tunnel results basically disagree.

Another rough evaluation of the single-faced baffle has been obtained through its use on blast lines on which corresponding ground stations were instrumented. In the far Mach region, where stem heights exceeded the elevation of the gauge, agreement between ground and air stations seems to have been satisfactory.[19,27] In these instances, however, the baffles were just nominally side-on, and little emphasis was placed on perfection of alignment or the tolerance to be observed.

It was therefore deemed worthwhile to attempt additional field checks of wind-tunnel results as a part of this study since a complete set of 18-inch square aluminum plates, machined to take the standard Wiancko gauge canister, was on hand. The scope of the orientation study was broadened to include baffles of several other configurations: several 18-inch circular baffles were specially fabricated, one having a butt edge and the remainder having different edge tapers; a square baffle having a tapered edge was also fabricated for trial on these tests. Comparative evaluation was planned to establish which combination of shape and edge geometry was superior should it be found that differences in measured pressures were of the magnitudes found by the Ballistic Research Laboratory[25] for their smaller pancake-type baffles and piezoelectric pressure-sensing elements.

When a baffle was yawed from the 6° position (assumed to be optimum on the basis of wind-tunnel tests), a 16-mm Fastax camera, running at a speed of 2000 frames/sec, was positioned to look along

the plane of the baffle and perpendicular to the ground. These cameras would, it was believed, detect any gross disturbance of flow by the baffle.

The yaw angles for all baffles used are listed in parentheses following the station designations in Table 2.2, the sign denoting upwind (+) or downwind (-) yaw. Upwind yaw is defined here as a yaw which turns the face of the baffle toward the charge. Since in nearly every instance free air pressure was to be measured, the yaw angle was determined by sighting along the face of the baffle to the charge, then rotating the baffle in that plane perpendicular to the baffle which contained the line of sight.

An unanticipated complication arose in the form of excessive ringing of the gauges. In earlier investigations in which the 17- or 18-inch baffles had been used with the Wiancko gauges the upper frequency limit of the intelligence recorded was 1000 cps or less, which is well below the mechanical resonant frequency of the gauges. However, the 20-kc carrier system used for this study had a flat frequency response from 0 to 3000 cps, and the resonant points for the 10- and 50-psi gauges, even of the 20PAD-WS type, are well within the recording range. Moreover, the low-pass filter circuit (App A), which is tuned to fix the flat response range, does not cut off sharply; hence the 3600-cps resonance of a 100-psi gauge will be seen with an attenuation of only 3-6 db. The baffle plates, set into vibration by the blast wave, supplied the driving force required to excite the gauge elements into resonance, and the recordings under such circumstances were unreadable.

Of the remedial measures tried in an effort to dampen these vibrations, the most practical seemed to be the attachment of lead weights at strategic points along three different radial axes (Fig. 2.7a) of the baffle. Single weights were placed one inch from the periphery of the baffle on each of the three axes, and a fourth was placed at the midpoint of one of these axes to forestall radial vibration. At best this method of damping proved only partially effective, however, and a laminated baffle that would be intrinsically well damped was designed and fabricated for trial during the latter part of the program. It was constructed of 18-inch square laminae of 1/4-inch aluminum plate and 1/4-inch lucite plate, separated by a paper gasket 1/32-inch thick and held together by means of screws (Fig. 2.7b).

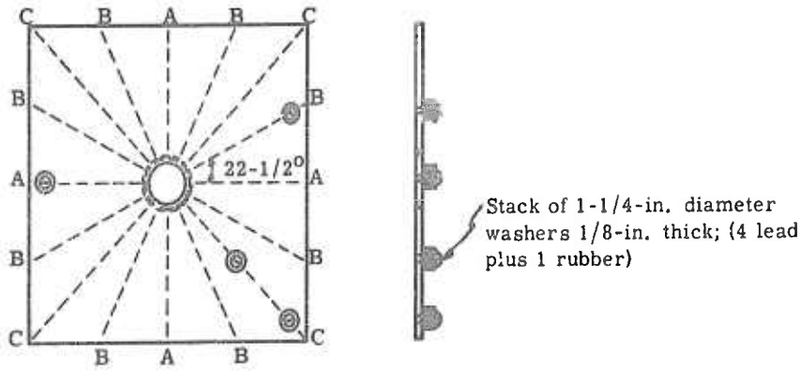

Fig. 2.7a

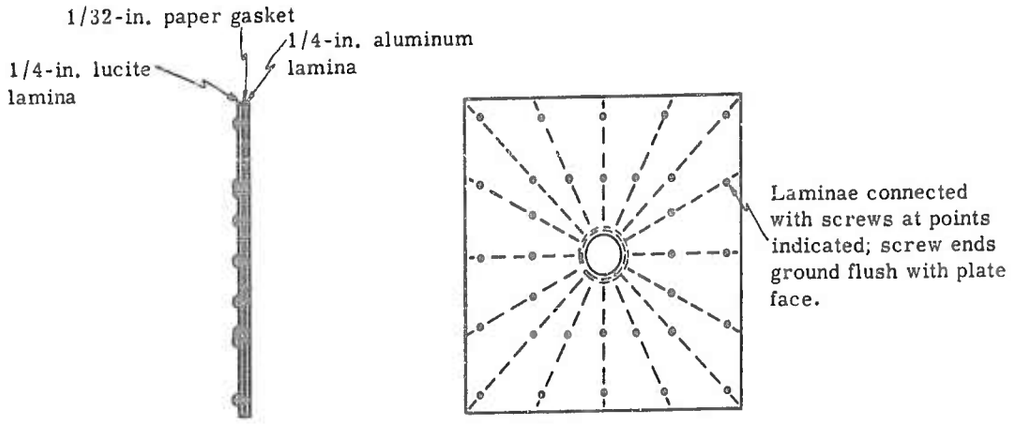

Fig. 2.7b

Fig. 2.7 -- Vibration Damping of Baffle Plates: (a) Simple Baffle with Damping Attachment; (b) Aluminum-Lucite Laminated Baffle

While this laminated baffle proved satisfactory, it was developed so late in the program that virtually no conclusions concerning the effects of baffle orientation were feasible. The attempted study, then, served only as a developmental program for proper instrumentation and as background for future work on this phase of the problem.

CHAPTER 3

HIGH-EXPLOSIVE CHARGES

3.1 ASSEMBLY

The high-explosive charges used were TNT spheres 20-1/4 inches in diameter having nominal weights of 256 pounds. The TNT was received in the form of hemispheres in which the pentolite booster charge had been cast in place (Fig. 3.1). Because of the danger of assembling and handling the charge when the detonator was in place, it was necessary, prior to assembly of the hemispheres, to enlarge the channel leading from the surface of the sphere to the detonator pit to permit insertion of the detonator after assembly. The assembly operation consisted in placing the two hemispheres face to face and tightening two circumferential aluminum bands about the sphere as shown in Fig. 3.2. At low burst heights, i.e., 5 feet or less, the detonator could be installed after the charge was in place for firing; at higher burst heights, of course, the detonator had to be placed before the charge was hoisted into position.

3.2 METHOD OF SUSPENSION

For surface bursts (at a height of one charge radius) the assembled sphere was placed in a wooden stand so designed that the only point of contact of the sphere with the ground was at ground zero. In the one instance in which a half-buried charge was burst, a pit having a maximum depth of one charge radius was dug, the center of the charge placed exactly at ground zero, and the pit backfilled around the sphere.

For bursts above ground level the charge was placed in a canvas sling (Figs. 3.3 and 3.5) by means of which it could be hoisted to the proper height. The cable and pulley system for hoisting the charge was supported by two 110-foot wooden poles spaced 100 feet apart and equidistant from ground zero on a line perpendicular to the blast line (Figs. 2.1 and 3.4). These poles were intentionally inclined at a slight angle such that the suspended charge, when hanging free, was offset from ground zero by approximately three feet in the direction of the

Fig. 3.1 -- TNT Hemispheres, Showing Pentolite Booster and Channel for Insertion of Detonator

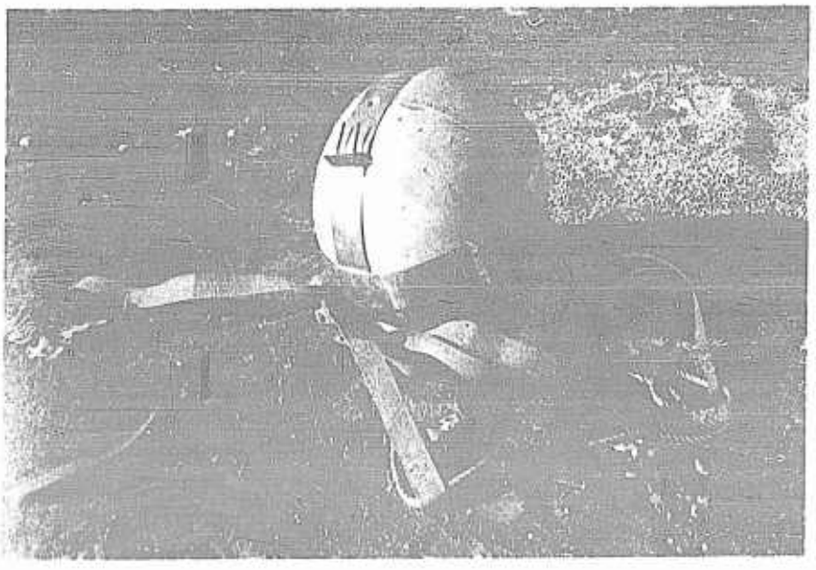

Fig. 3.2 -- Hemispheres Assembled, Held in Place by Means of Aluminum Bands. Note opening near top for insertion of detonator. When the sphere is in position for firing, the interfacial plane of the hemispheres is perpendicular to the blast line and the detonator channel is vertical, having its opening at the top.

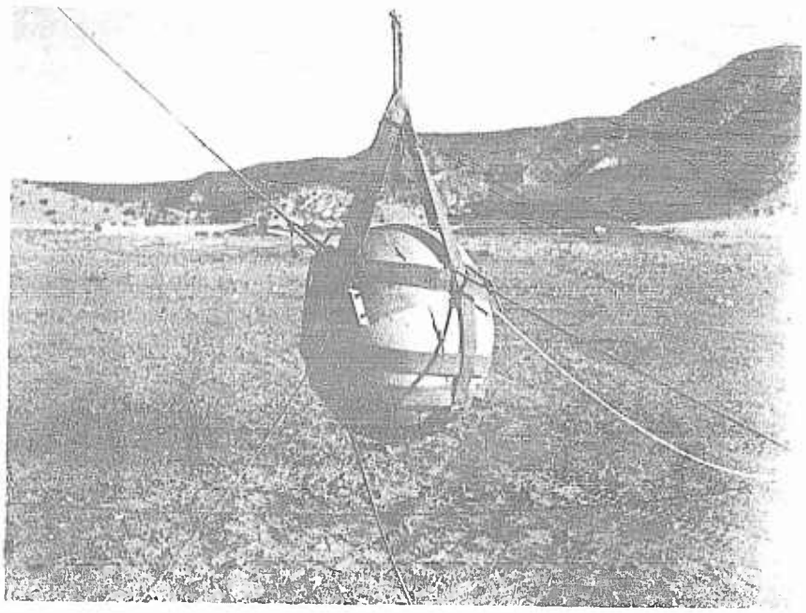

Fig. 3.3 -- Charge in Canvas Sling, with Guy Ropes in Place for Positioning Charge over Ground Zero

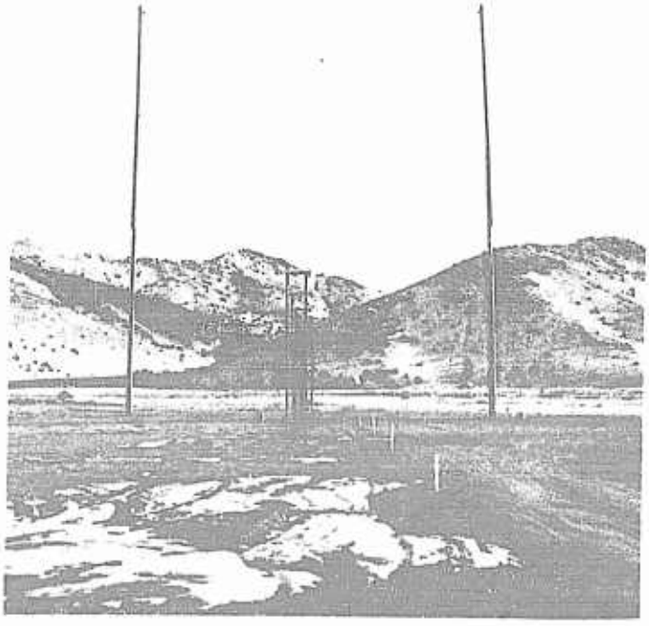

Fig. 3.4 -- View of Blast Line Looking toward Ground Zero, Charge in Place. Note rigging of suspension poles. Cables to gauges appear in foreground.

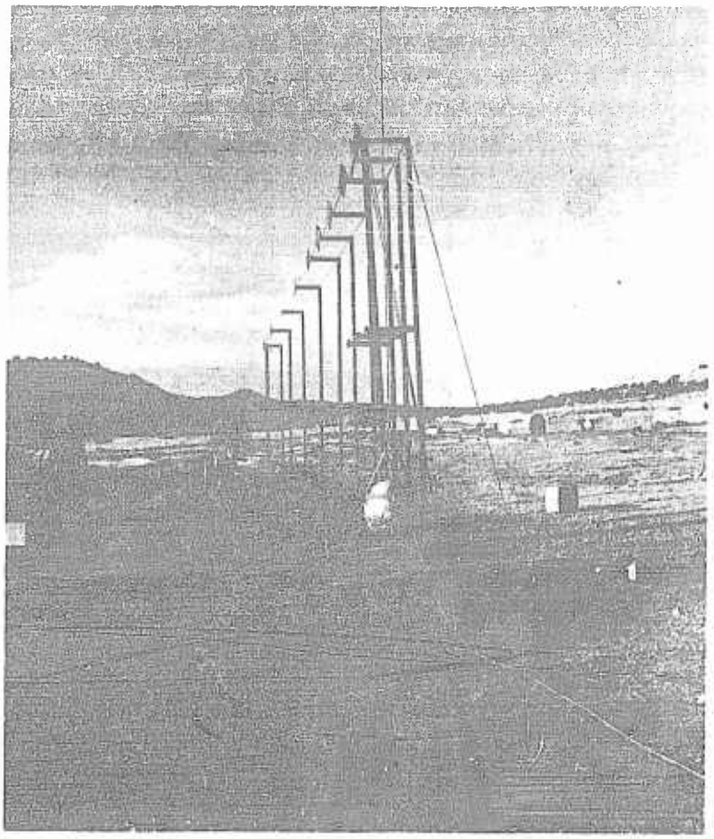

Fig. 3.5 -- View of Blast Line from Ground Zero, Showing Charge Hoisted to Proper Height

blast line. By means of a system of cotton guy lines attached at three points about the horiztonal circumference of the sphere it could be positioned directly above ground zero and held in place until time for detonation. Alignment was carefully checked by use of surveyor's transits.

The detonators used were electrically fired, and for the bursts at heights above ground level the leads to the detonators were supported by the suspension poles.

Fastax motion picture studies of the growth of the fireball, taken at a speed of 10,000 frames/sec, provided valuable information on jet formation and the shape of the blast wave in the early phases. Colored motion pictures were taken at speeds of 1000 and 200 frames/sec on Shot 39.

CHAPTER 4

DISCUSSION OF RESULTS

In tracing the history of the height-of-burst problem no mention was made of the tremendous amount of small-charge experimentation subsequent to that of Stoner and Bleakney.[8] This omission was purposeful in that the high-explosive studies during this period had a small, if not negligible, role in actually shaping the height-of-burst curves. It will be remembered that the pressure-time and pressure-distance data from Operations SANDSTONE, GREENHOUSE, BUSTER, and TUMBLER were at variance with even the most imaginative extrapolations from data obtained using chemical explosives. Nevertheless experimental programs using chemical explosives were continued, resulting in an accumulation of significant fundamental information. A number of them form a background against which to discuss the present experimental program using 250-pound TNT charges and in that role merit brief mention here.

One of the most noteworthy of these earlier studies was the experimental determination by Fisher[29] of the free-air curve for centrally detonated 8-pound TNT spheres, in which he used measured shock velocities to reckon overpressures. This study paralleled the work of Stoner and Bleakney in which pentolite spheres were used, and the results were an excellent experimental corroboration of the Kirkwood-Brinkley[9] theoretical free-air curve for TNT in the overpressure range of 5 to 50 psi. At about this time a translation of a Swedish publication on the same subject was published by the Ballistic Research Laboratory.[30] This investigation by Weibull was aimed at determination of shock velocities as a function of distance; however, these data, when converted into overpressure-distance information by Hartmann,[31] agreed well with the Kirkwood-Brinkley curve for the overpressure range of 1 to 1000 psi. Thus, with the joint experimental support of these two studies, the theoretical curve for TNT was well established.

Several additional investigations using chemical explosives followed in close sequence, the majority of them undertaken by the Naval Ordnance Laboratory and the Ballistic Research Laboratory.

Image-charge experiments simulating a perfect reflecting plane were performed to give a sound basis for evaluating different actual reflecting surfaces.[31, 32] Pressure-distance relations along the ground and vertically above the charge were measured for surface bursts and bursts at elevations of one and two charge radii[33] in an effort to determine the influence of proximity to the reflecting surface and the extent of energy diversion into cratering and ground shock. Sachs' formulas[34] for altitude correction of pressure-distance data from one homogenous atmosphere to another were given experimental support in the range from sea level to a simulated altitude of 50,000 feet.[35] The earlier work of Stoner and Bleakney in determining the free-air curve for pentolite was repeated using direct pressure measurement in lieu of the shock-velocity method for determining overpressures.[36] Pressure-time profiles and such related quantities as positive and negative phase durations as well as partial and total impulses and blast-wave energies were determined. All these studies were carefully instrumented, and the results stand as important contributions to the fund of basic experimental knowledge of blast waves.

The most recent and certainly the most comparable investigation is the optimum height-of-burst study reported by Hartmann of the Naval Ordnance Laboratory.[37] This study, in which 1-pound centrally detonated pentolite spheres were burst over a concrete reflecting plane, was really the first complete height-of-burst study using high explosives; it parallels exactly the work of Sandia Corporation reported here, in which 250-pound TNT spheres were used.

If the results of the two investigations are to be critically compared, some details of the technique employed by NOL must be discussed. As was just pointed out, NOL worked with 1-pound centrally detonated spheres, bursting them over a concrete slab. The pressure-sensing elements used were piezoelectric gauges dynamically calibrated* during the tests. They were mounted in baffles oriented side-on to the blast; the centers of the gauges were at a reduced height of 0.18 ft/lb$^{1/3}$. The above-ground locations of these gauges obviously had an important bearing on the measurements. In the region of regular reflection, where the reflected wave is displaced in time for any location off the ground, these gauges read the peak attained after arrival of the reflected

*By comparison with velocity-switch pairs, the piezoelectric gauge being positioned midway between the switches.

wave; the usual 'gauge size' correction[38] was applied to get the overpressure reading, and the step rise was ignored. Thus one would expect this reading to differ from that of a ground baffle gauge such as was used by Sandia, at which the incident and reflected waves occur simultaneously and the true reflected overpressure is seen. This difference is most pronounced directly beneath the charge (as is stated in the NOL report) and decreases continuously until the Mach stem grows to a height such that it encompasses the air baffle gauge completely. Ideally the readings from the ground baffle and the side-on baffle should be the same at this point and beyond. However, any attenuation of the blast wave as a result of surface roughness will be manifest to a greater degree at ground level than at points above ground level. Moreover, for a given gauge height the effect should, it seems, be more pronounced the slower the rate of Mach stem growth, i.e., the higher the burst height.

The effects on blast wave propagation of various degrees of surface roughness have been reported by several investigators.[39,40,41] In general, increasing retardation of the Mach stem in contact with the surface was noted with increasing surface roughness, and extreme roughness was found[39] to cause complete degeneration of the Mach stem. While the degrees of surface roughness present in the Sandia and NOL experiments doubtless fall within the range of surface roughness tested by Duff in his shock-tube study,[40] application of his quantitative results to exponential blast waves is extremely difficult. Certainly his results give qualitative corroboration of the explanation offered above for discrepancies between the Sandia and NOL data in the early Mach region. Further corroborative evidence is found in the comparison[41] of Mach stem growth over hard-packed dirt and dry sand.

An attempt was made on Shots 42 and 43 (Tables 4.1 and 4.2) of this series to estimate the influence of surface roughness by instrumenting a double blast line, consisting of a string of ground baffles and a corresponding array of side-on air baffles at a reduced height* of approximately 0.25. Since only two shots were fired using this blast-line configuration and large burst heights, no quantitative evaluation of results was possible. However, on both shots, at reduced heights of about 10.2 and 11.7 (TNT), the air baffle gauges recorded the higher overpressures in the Mach region. Certainly the paucity of data dictates caution in drawing conclusions, and it is merely suggested that

*This reduced height is about that of the upper edges of the NOL gauges.

TABLE 4.1

Measured Peak Overpressures (psi) at Ground Level

Gnd Distance (ft) \ HOB / Shot	0 ft	1 ft		
	46	29	30	Av
0	-	-	-	-
5	-	-	-	-
10	-	-	-	-
15	-	-	-	-
20	-	-	-	-
25	35	-	-	-
30	-	50	46	48
35	20	45	31	38
45	9.0	20	16.2	18.1
55	6.5	12.2	11.5	11.8
65	5.8	9.0	8.8	8.9
85	3.9	5.8	5.1	5.4
110	1.80	3.3	3.2	3.2
135	1.80	2.30	2.20	2.20
160	1.20	1.80	1.80	1.80
190	-	1.30	1.26	1.28
225	0.80	1.16	1.08	1.13
275	-	0.87	0.90	0.88

TABLE 4.1 (cont)

Gnd Distance (ft) \ HOB / Shot	2 ft	5 ft	15 ft			
	45	44	28	31	31R	Av
0	-	-	-	-	-	-
5	-	-	-	-	-	-
10	-	-	-	-	-	-
15	-	-	-	-	-	-
20	-	-	122	140	100	121
25	45	66	100	95	77	91
30	-	-	62	68	-	65
35	29	38	45	-	-	45
45	11.6	13.4	21.2	24.5	-	22.8
55	9.2	11.0	14.5	-	10	12.3
65	8.0	9.5	12.0	11.1	8	10.4
85	4.7	5.2	7.1	6.2	5.3	6.2
110	2.30	2.80	3.8	4.9	-	4.4
135	2.00	2.10	3.0	3.5	-	3.3
160	1.35	1.60	2.30	2.80	2.00	2.40
190	-	-	1.52	1.60	1.20	1.43
225	0.86	0.98	1.43	-	-	-
275	-	-	1.15	-	-	1.15

TABLE 4.1 (cont)

Gnd Distance (ft) \ HOB / Shot	20 ft	25 ft	30 ft	35 ft			
	27	26	25	24	32	33	Av
0	-	-	73	48	75	104	76
5	-	-	-	-	-	-	-
10	-	-	-	58	-	44	51
15	-	-	-	-	60	-	-
20	-	70	58	60		36	48
25	-	74	54	36	36	-	36
30	48	47	49	16	-	27	21.5
35	32	44	37	14	24.5	23	20.5
45	21	22	25	15.0	15.8	18	16.3
55	13.0	15.1	14.5	13.0	12.6	15.0	13.5
65	9.3	12.5	10.6	10.7	11.0	12.5	11.4
85	6.3	8.4	7.0	7.0	7.5	8.2	7.6
110	4.0	4.7	4.7	4.1	5.4	5.3	4.9
135	2.50	2.80	3.5	3.4	3.5	3.3	3.4
160	2.15	2.45	2.10	2.80	2.46	2.60	2.62
190	1.40	1.53	1.75	1.85	-	-	1.85
225	1.30	1.50	1.50	1.75	-	-	1.75
275	1.00	1.20	1.30	1.43	-	-	1.43

TABLE 4.1 (cont)

Gnd Distance (ft) \ HOB / Shot	40 ft				45 ft		
	23	34	35	Av	22	36	Av
0	58	35	42	45	35	36	36
5	-	-	-	-	-	-	-
10	-	37	-	37	31.5	39	35
15	-	-	-	-	-	-	-
20	28	34	31	31	25.5	-	25.5
25	-	-	-	-	21	20	20.5
30	25	25.4	23.2	24.5	18.5	-	18.5
35	18.5	-	-	18.5	20	18	19
45	-	15.0	16.5	15.8	-	17.3	17.3
55	13.3	13.0	14.1	13.5	15.5	13.2	14.2
65	10.7	11.5	13.0	11.7	12.0	12.0	12.0
85	6.5	7.0	7.8	7.1	7.6	7.6	7.6
110	4.7	6.3	4.5	5.2	-	5.9	5.9
135	3.5	3.7	3.6	3.6	4.3	3.6	4.0
160	2.60	2.76	2.70	2.60	3.6	-	3.6
190	1.86	-	-	1.86	2.52	-	2.52
225	1.78	-	-	1.78	2.20	-	2.20
275	1.46	1.17	1.12	1.25	1.54	-	1.54

TABLE 4.1 (cont)

Gnd Distance (ft) \ HOB / Shot	50 ft			55 ft	60 ft	70 ft		
	21	37	Av	38	20	15	42	Av
0	22	22	22	22.5	16.6	11.3	-	11.3
5	-	-	-	-	-	11.5	-	11.5
10	24.6	-	24.6	-	16.8	10.6	-	10.6
15	-	23	23	23	17	11.5	-	11.5
20	21	-	21	-	-	12.0	-	12.0
25	20.8	21.2	21	16	13.0	10.3	-	10.3
30	17.2	-	17.2	-	11.8	11.3	-	11.3
35	17.0	18	17.5	11.5	11.0	10.4	7.5	9.0
45	-	13.8	13.8	14.0	11.6	-	7.5	7.5
55	11.6	11.0	11.3	10.2	10.1	-	7.9	7.9
65	10.5	8.9	9.5	-	-	7.0	7.3	7.2
85	7.2	7.7	7.5	7.1	6.9	6.1	5.0	5.6
110	-	5.8	5.8	5.9	-	4.5	3.6	4.1
135	3.9	3.6	3.8	3.3	3.7	3.1	3.3	3.2
160	3.3	3.1	3.2	2.14	3.2	2.80	2.60	2.7
190	2.15	2.40	2.28	2.12	2.20	2.10	-	2.10
225	1.90	2.00	1.95	-	2.05	1.90	-	1.90
275	1.32	1.30	1.31	-	1.60	1.80	-	1.80

TABLE 4.1 (cont)

Gnd Distance (ft) \ HOB / Shot	80 ft				90 ft	100 ft
	13	14	43	Av	16	18
0	10.1	8.6	-	9.4	7.7	6.6
5	-	9.0	-	9.0	8.1	6.9
10	10.0	9.8	-	9.9	8.2	6.7
15	-	10.9	-	10.9	8.9	7.6
20	9.5	11.0	-	10.3	8.0	7.0
25	-	9.3	7.3	8.3	6.8	5.9
30	-	10.6	-	10.6	7.4	6.3
35	9.0	9.8	6.1	8.3	7.2	6.0
45	8.5	-	6.2	7.4	-	5.8
55	5.9	-	6.5	6.2	-	-
65	-	6.3	6.1	6.2	5.9	4.8
85	-	5.2	4.4	4.8	4.9	4.2
110	3.9	4.0	3.2	3.7	3.6	3.2
135	-	3.3	3.0	3.2	3.4	3.0
160	3.1	2.90	2.60	2.90	2.90	2.60
190	2.50	2.20	-	2.35	2.20	-
225	2.10	1.90	-	2.00	2.10	2.00
275	1.80	1.70	-	1.75	1.60	1.35

TABLE 4.2

Measured Peak Overpressures (psi)
(1.5 ft above ground level)

Gnd Distance (ft) \ HOB / Shot	0 ft	2 ft	5 ft	70 ft	80 ft
	46	45	44	43	42
25	-	-	-	7.8	6.0
35	16	18.6	31	7.3	6.1
45	10.2	14.7	18	6.9	5.8
55	6.7	9.6	11.8	7.1	5.8
65	5.9	7.6	8.6	6.6	5.4
85	3.6	4.6	5.4	6.4	4.7
110	2.30	2.90	3.1	4.0	3.5
135	1.74	2.06	2.40	3.3	3.0
160	1.35	1.53	1.88	2.90	2.70

surface roughness could have contributed to the disagreement of the NOL and Sandia data for lower overpressures and large burst heights.

The results of all measurements of overpressure in the Sandia experiments with 250-pound TNT spheres are presented in Tables 4.1 and 4.2. The former lists ground-level measurements, the latter overpressures measured using side-on baffles 1.5 feet above ground level. As mentioned earlier, attempted measurements of free air pressures and spot checks of Mach stem growth were considered invalid in the face of excessive gauge ringing and spurious responses of large amplitude and hence do not merit inclusion. Considerable scatter will be noted among measured overpressures of 20 psi and above. It is believed that these discrepancies are principally the effects of large jets emanating from the TNT charges despite their sphericity. In all seven Fastax films (>10,000 frames per second) of fireball growth, jets were both prominent and abundant (frontispiece). Pressure-time records from ground baffles on several shots supported this explanation by exhibiting step rises which indicated that premature shocks of one-third to one-half the main shock amplitude arrived as many as 3 msec in advance of the main shock.

The averaged data (ground level measurements) in Table 4.1, smoothed graphically, and reduced to sea level and 1 pound of TNT, are plotted in Fig. 4.1. The set of points at each height defines the measured pressure-distance curve for that burst height. To facilitate comparison the NOL curves are superposed on this height-of-burst chart. In addition to the expected differences at large burst heights, there are discrepancies at very low burst heights; particularly conspicuous are the dissimilarities in shape at reduced heights, μ, of less than 1 ft/lb$^{1/3}$. Unfortunately the NOL study included no shots at heights less than $\mu = 2$ (about 15 charge radii) aside from the actual surface bursts. Their curves were extended across this gap by assuming the simplest type of transition. An earlier NOL publication, [33] however, had treated a careful exploration of pressure-distance phenomena from charges burst at heights of zero, one, and two charge radii. These results evinced a rapidly increasing air blast efficiency as the charge was separated from the ground. Free-air equivalent weight ratios at the 10- and 20-psi levels, for instance, were found to increase from 0.82 and 0.66 for surface bursts to 1.52 and 1.59 for bursts two charge radii above the ground. In the light of these results it is evident that the isobars must turn back sharply as they approach zero height.

Just such behavior is indicated by the data obtained by Sandia on Shots 44-46, at reduced heights of zero, 0.31, and 0.78. These three sets of points, each the result of a single shot, were obtained on the same day under practically identical soil conditions -- a thawing surface with patches of melting snow on the ground. The set of points for $\mu = 0.16$ (about one charge radius) was derived from the average data from two shots (29 and 30), both fired when the surface was firm and dry. Differences between this set of points and the three sets mentioned earlier are construed as evidence of the strong dependence of the amount of energy going into air blast upon the condition of the soil, which interacts with the fireball of the explosion. It seems likely that the complexity of the phenomena involved when bursts are low enough to cause cratering is such that a large variability in the shapes of the isobars in this height range is to be expected. Certainly much additional experimentation is needed if the limits of this variability are to be established. Nevertheless, on the basis of existing information,

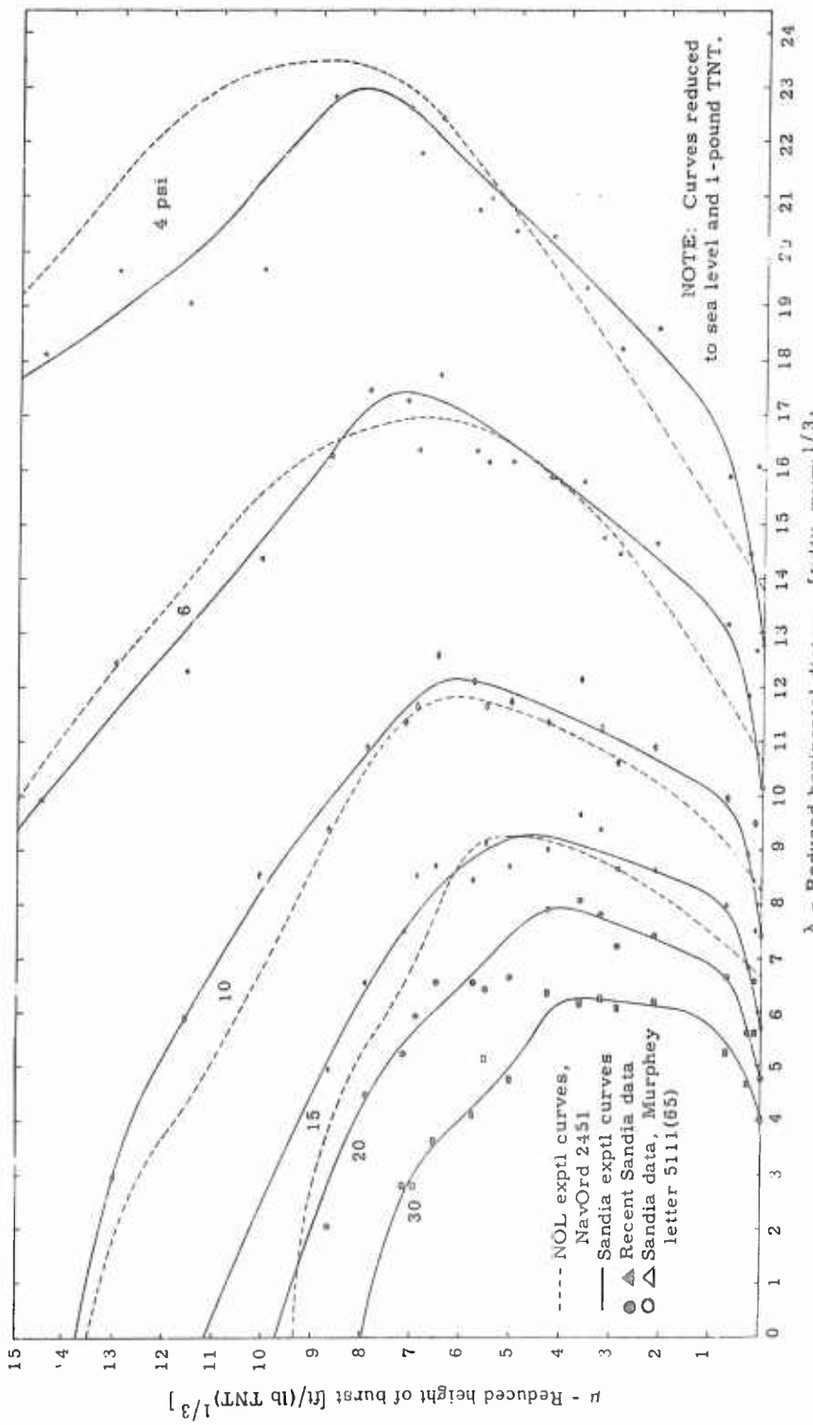

Fig. 4.1 -- Data and Inferred HOB Curves for 250-lb TNT Spheres

the pronounced bend at the foot of each isobar as derived from Sandia data seems more realistic than the simpler shape of the NOL curves.*

It seems apparent that only continued work on the problem can resolve or explain the several differences noted between the two sets of curves. No marked changes are anticipated from such a continuation. It is believed that both the NOL and Sandia height-of-burst curves can be used with confidence, although the Sandia curves appear to be more accurate in the region below $\mu = 1$ ft/lb$^{1/3}$ for the reasons discussed. To permit better reference to the Sandia curves, they are replotted on a full grid in Fig. 4.2.

While the height-of-burst chart is the simplest method of presenting the data from experimental studies of this sort for practical application, it gives little insight into details of the reflection process. Early semiempirical treatments of the height-of-burst problem[11,12,14] incorporated all assumptions and reasoning into a reflection chart; the height-of-burst curve was devised merely as an application of this fundamental information to a specific free-air curve. Thus comparison of recent work with that of early investigators is best done on the basis of a reflection chart; such a chart (Fig. 4.3) was constructed using reflected overpressure data from the 250-pound TNT shots and the theoretical free-air curve of Kirkwood and Brinkley. Dissatisfaction with the free-air curve measured during the experiments with 250-pound TNT charges† prompted use of the theoretical curve.

---

*On February 9, 1953, a conference attended by C. J. Aronson, W. E. Morris, J. F. Moulton, E. M. Fisher, P. Z. Kalavski, and the author was held at the Naval Ordnance Laboratory at White Oaks, Maryland. At that time the NOL group agreed to this point.

†The unfortunate choice of a burst height of 35 feet and gauge elevations of 20 feet made the reflection times too short at the outlying stations to permit accurate determination of incident peak pressures. Furthermore, the problem of ringing of the gauges, induced by vibration of the baffles, had been only partially solved at this time, and the records exhibited oscillations of objectionable amplitude. As pointed out earlier, pressure of additional programs at the Coyote Canyon test site made immediate repetition of the free-air pressure measurements impossible.

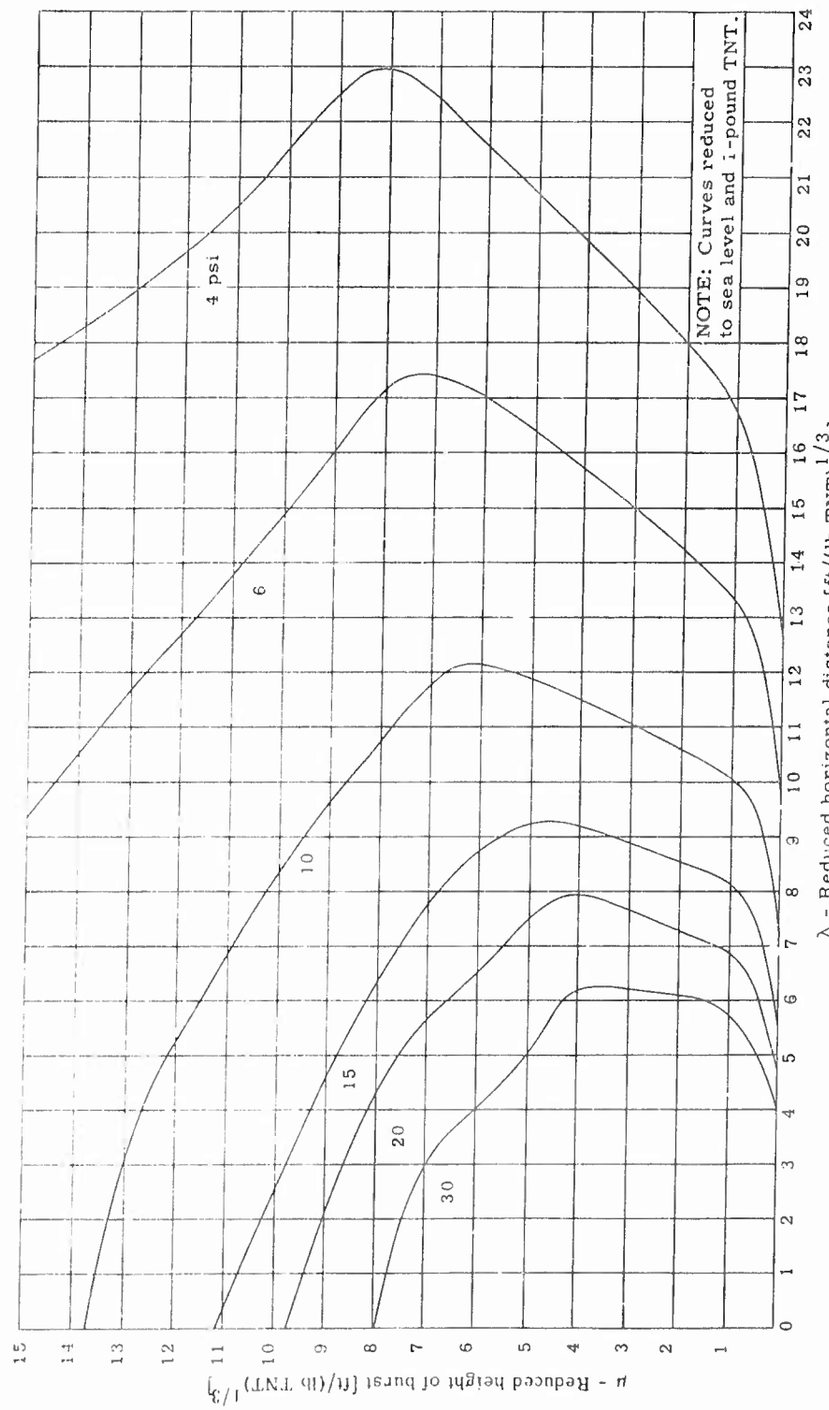

Fig. 4.2 -- HOB Curves Inferred from Study Using 250-lb TNT Spheres

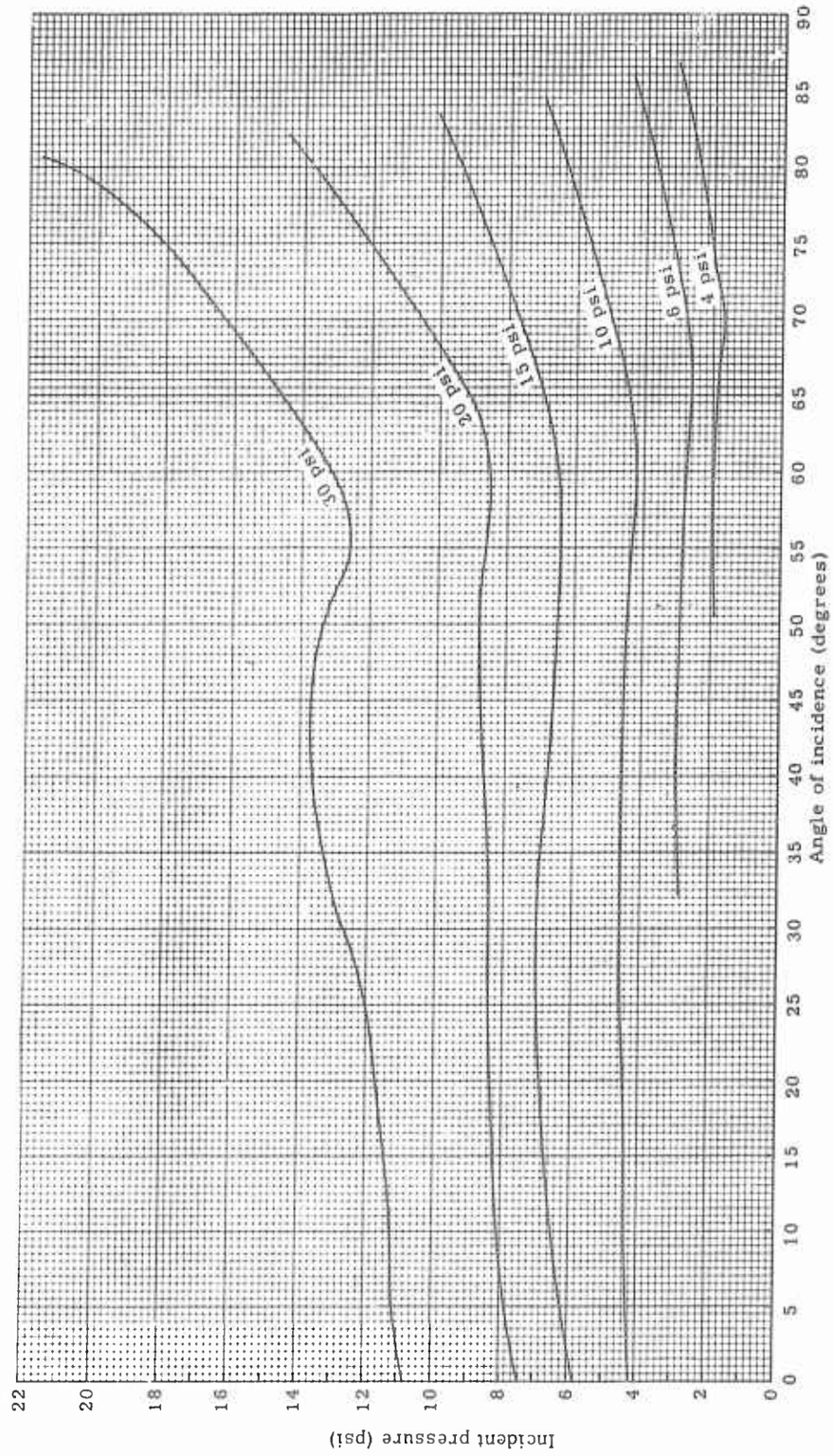

Fig. 4.3 -- Reflection Chart (Based on 250-lb TNT Spheres and Kirkwood-Brinkley Free-Air Curve)

Note that none of the isobars (Fig. 4.3) has been carried to glancing incidence (90°). In view of the variability that characterizes the height-of-burst curves in the region below $\mu = 1$ ft/lb$^{1/3}$, the belief was that no information in this range merited inclusion.

In Fig. 4.4 the 15-psi isobar from Fig. 4.3 has been replotted with the corresponding isobars after Porzel-Reines[11] and Pelsor-Prim[14]. The dissimilarities are sizeable indeed, the most conspicuous being those in the final stages of regular reflection and in the early Mach region. An explanation of this deviation has been offered elsewhere.[42] It is believed that pressure multiplications of the magnitudes predicted by these early reflection charts would require large additions of energy to the blast wave if the usual pressure-time profile were to obtain. Since there is no conceivable source for the required energy, it is concluded that these large predicted peak pressures can exist only as short-duration pressure spikes at the shock front. At two of the 15-foot air baffle stations on the blast line for BUSTER Shot Baker such pressure spikes -- 1 to 2 per cent of the positive phase duration -- were recorded[17] by four gauges, and their amplitudes were in fair agreement[42] with the Porzel-Reines curves. It is unlikely that any such spike occurring on the 250-pound TNT explosions could have been resolved by the instrumentation used for these measurements, and none was observed.

In the far Mach region the 15-psi isobar for the 250-pound charges courses about midway between those of Porzel-Reines and Pelsor-Prim. This fact is interpreted to mean that the surface roughness of the test site was significant for a charge weight of 250 pounds. The dip in the curve at the extreme left (normal incidence) shows an inexplicable violation of regular reflection theory; hence this short segment is viewed with suspicion.

In that the primary interest here is the predictability of effects from nuclear explosions, the most important critique of any height-of-burst study using chemical explosives becomes the manner in which the small-scale results correlate with those derived from nuclear blast tests. In Fig. 4.5 the NOL and Sandia curves are scaled to 0.5 KT of TNT, which is assumed to be equivalent to a nuclear radiochemical

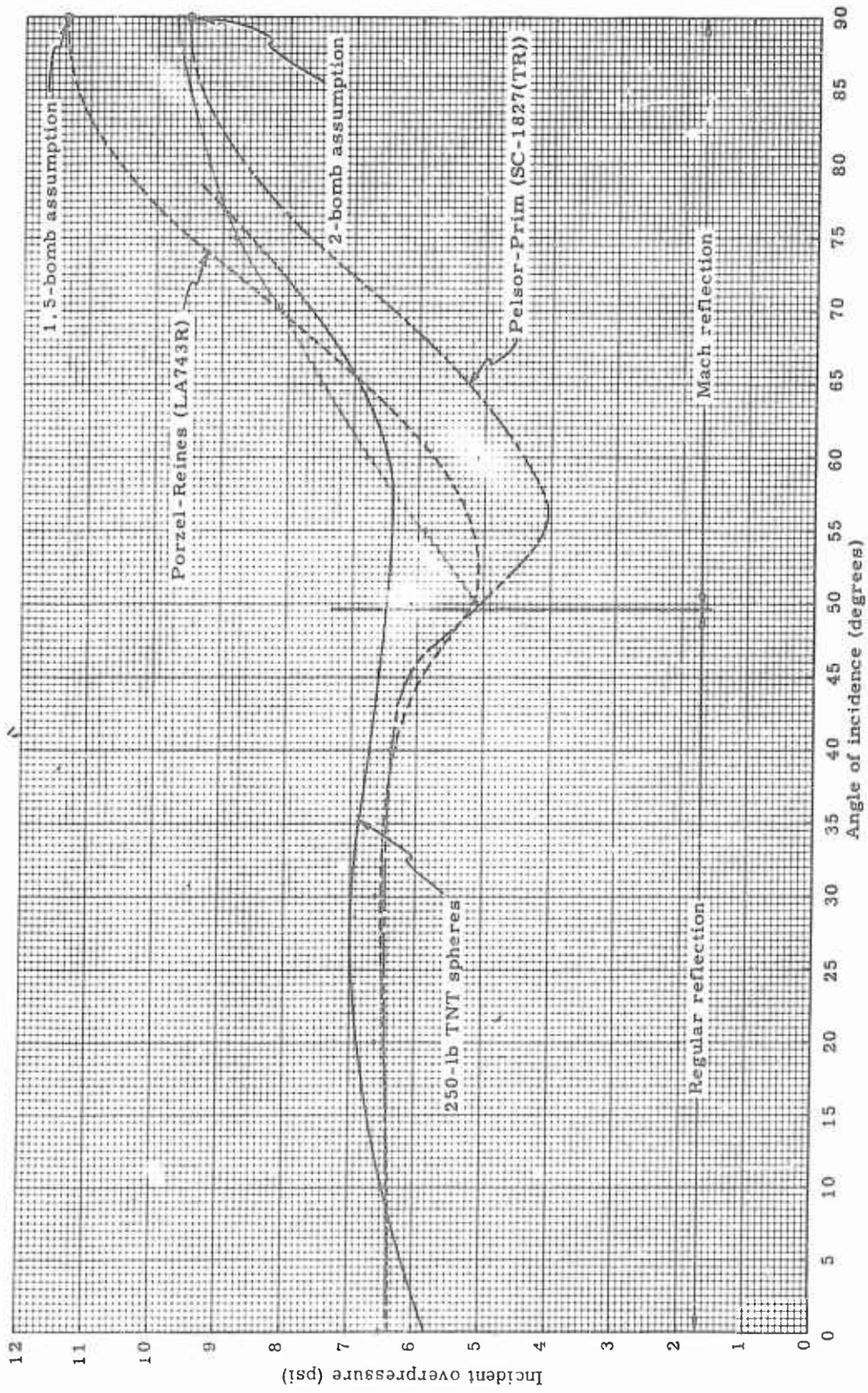

Fig. 4.4 -- Comparison of Reflection Charts from Three Sources at the Reflected Overpressure Level of 15 psi

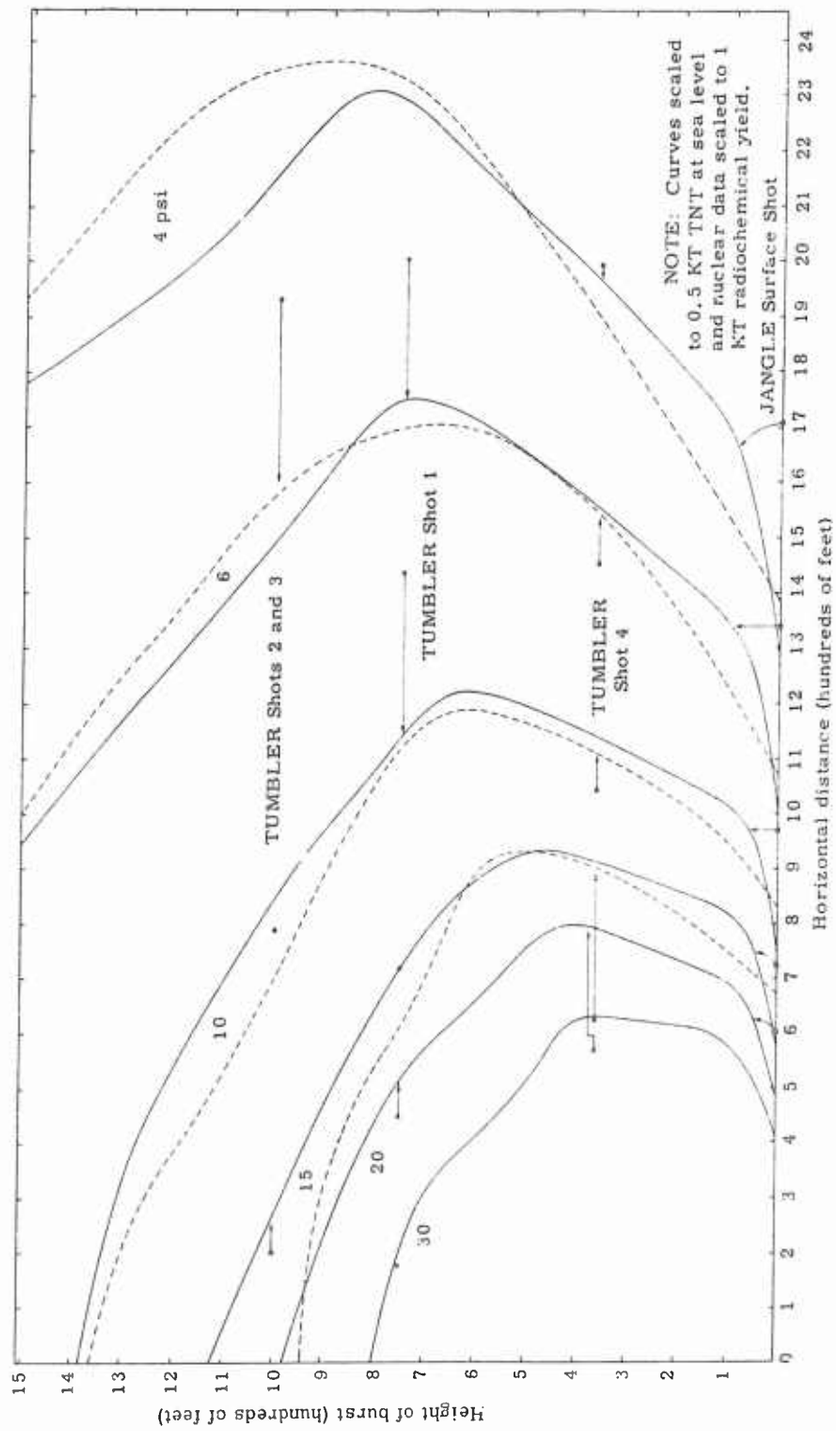

Fig. 4.5 -- Comparison of NOL and Sandia HOB Curves with Recent Nuclear Test Data

yield of 1 KT of TNT. While the best average blast efficiency for the TUMBLER shots is reported[22] to be 0.44, that published for the JANGLE surface shot was 0.78 and the average[31] for the GREENHOUSE shots was 0.60. The simple value of 0.50 used for Fig. 4.5 weighs the TUMBLER results heavily but admits some influence from the JANGLE and GREENHOUSE results. Superposed on the curves are averaged data from TUMBLER Shots 2 and 3, data from both TUMBLER Shots 1 and 4, and the data from direct pressure measurements* on the JANGLE surface shot.[21] The arrows attached to various data points indicate the pressure level of the point by choosing the pertinent pair of isobars. These particular results are chosen for comparison because they represent extremes in burst height and thermal level as well as one intermediate set of conditions to aid in marking the nature of the transition between extremes. From the results of the surface shot one concludes that there is little degradation of the air blast energy from a nuclear device despite the work of cratering and the creation of energetic earth shock. This conclusion stands in sharp contrast to experience with HE surface shots. To be more specific, the free-air equivalent weight ratio for the JANGLE surface shot appears to have varied between 1.5 and 2.0, i.e., the data lay between the 1.5- and 2-bomb assumptions. The zero-height intercepts for the NOL curves may be used as a reference, for they represent points from the Stoner-Bleakney free-air curve in terms of TNT. The 2-bomb assumption merely shifts each pressure to a distance 26 per cent beyond that of the pertinent intercept of the NOL curve, while the 1.5-bomb assumption increases all distances by about 11.5 per cent.

One general difference noted from a comparison of the nuclear and HE curves is that, within the limits of thermal levels and burst heights considered, the distances to the 4-psi level for the nuclear shots exceed those predicted from the curves for the high-explosive shots. In fact, the 4-psi points for TUMBLER Shot 1 and TUMBLER Shots 2 and 3 were outside the confines of this chart, being at 2600 and 2800 feet, respectively. In contrast, the curves for the high-explosives data approximated fairly closely those points obtained from TUMBLER Shots 2 and 3 for the 10- and 15-psi levels and the TUMBLER 1 points for 15, 20, and 30 psi. On the other hand, extreme discrepancies are

*Pressures reckoned from blast-switch data[43] were noticeably higher than these. However, the two sets of observations converge at about 4 psi and are in agreement at lower pressures.

noted at pressure levels of 10-psi and above with data from TUMBLER Shot 4, which had a prominent precursor, presumably the result of intense thermal radiation. Obviously curves obtained from bursts of chemical explosives cannot be expected to take cognizance of anomalies caused by thermal radiation. Even the data from TUMBLER Shot 4 cannot be taken as representative for that particular scaled height of burst. The present explanation of precursor formation pictures virtually a threshold surface effect; hence a bomb of very small yield burst at the scaled height of TUMBLER Shot 4 may cause no precursor and as a result give pressure-distance data more nearly in agreement with the high-explosives information.

Conversely, the blast wave from a nuclear explosion much larger than TUMBLER Shot 4 but at the same scaled height would undergo undue attenuation out to slightly lower pressure levels than on TUMBLER Shot 4. The fact that the waveforms from TUMBLER Shot 4 showed gross distortions magnifies the inapplicability of the height-of-burst curves from high-explosive shots in this height range. Obviously the damage capability of a steep-fronted blast wave of 20-psi peak overpressure cannot be compared directly with that of a misshapen blast wave of the same peak overpressure, particularly when the peak is reached as late as the middle of the positive phase. In truth, the manner in which such a comparison can be effected is an unanswered question of considerable consequence.

CHAPTER 5

CONCLUSIONS AND RECOMMENDATIONS

In the light of the comparisons drawn it must be admitted that height-of-burst curves derived from high-explosive charges of 250 pounds or less inherently fall short of direct applicability to nuclear explosions over land. Possibly data from nuclear shots over water would be in better agreement with these curves, although even this expectation seems untenable on the basis of the disagreement, at lower pressure levels, between these curves and the averaged data from TUMBLER Shots 2 and 3, on which thermal levels were comparatively low. But the pointed inadequacies of the height-of-burst curves based on high-explosives data in this connection should not be interpreted to mean that the studies by Sandia Corporation and the Naval Ordnance Laboratory have served an empty purpose. On the contrary, they served an extremely worthwhile purpose in their better definition of the limitations of small-scale experiments for predicting effects from nuclear explosions. Too, the height-of-burst information certainly is directly applicable to a wide range of weights of chemical explosives.

While the pitfalls of extrapolating height-of-burst data from high explosives to nuclear weapons will apparently always exist, a broad field of endeavor for small-charge experiments remains. Several specific avenues of investigation have suggested themselves in the course of this study, and the ideas involved are offered for appraisal.

Since subtle differences in surface texture, such as those between hardpacked dirt and dry sand, evidently exert a measurable influence on the growth of the Mach stem, [41] it appears that an ivestigation, similar in gamut and caliber to that of the shock-tube studies of Duff, [40] should be made for spherically divergent blast waves.

Existing data on growth of the Mach stem from a blast wave evince considerable disagreement. This disagreement apparently is not confined to small-scale studies, for similar discrepancies appear in available full-scale data. Perhaps a better understanding of the contributions of surface roughness will help resolve present differences.

There is also a need for useful information on the advanced stages of Mach stem growth, i.e., from measured heights to near completion of a 'Mach hemisphere.' This information is of considerable importance in predicting damage to delivery aircraft from nuclear explosions.

Finally, it seems desirable to have a dependable empirical description of the efficacy of single-faced side-on baffles. Sandia Corporation intends to resume this study as soon as the Coyote Canyon test site is available.

LIST OF REFERENCES

1. The Effect of the Height of Burst at Which a Bomb Explodes on the Blast Pressures, Road Research Laboratory (Br) note No. ARP/255/RJ, August 1941; General Estimate of the Results of Experiments with the Model Town, Ministry of Home Security (Br) note No. REN 110, August 5, 1941

2. von Neumann, J., Oblique Reflection of Shocks, Navy Department Bureau of Ordnance Explosives Research report No. 12, October 12, 1943

3. Kennedy, W. D., The Effect of Air-Burst on the Blast from Bombs and Small Charges, Experimental Results (Vol I) (report on work done by the Underwater Explosives Research Laboratory in collaboration with the Stanolind Oil and Gas Co), National Defense Research Committee report No. OSRD-4246, September 18, 1944

4. Halverson, R. R., The Effect of Air-Burst on the Blast from Bombs and Small Charges, Analysis of Experimental Results (Vol II) (report on work done by the Underwater Explosives Research Laboratory), National Defense Research Committee report No. OSRD-4899, April 6, 1945

5. Taub, A. H., Peak Pressure Dependence on Height of Detonation, National Defense Research Committee report No. OSRD-4076a, August 1944; Stoner, R. G., and Taub, A. H., Impulse Dependence on Height of Detonation, National Defense Research Committe report No. OSRD-4147c, September 1944; Kennedy, W. D., and Arentzen, R. F., The Effect of Height of Detonation on Peak Pressure and Positive Impulse Measured Close to the Ground, National Defense Research Committee report No. OSRD-4514d, December 1944

6. Air Burst for Blast Bombs (symposium), National Defense Research Committee report No. OSRD-4943, April 17, 1945

LIST OF REFERENCES (cont)

7. Blast Wave (Ed by H. A. Bethe), Vol III, Los Alamos Scientific Laboratory report No. LA-1021, August 13, 1947, Ch 10 (by von Neumann and Reines)

8. Stoner, R. G., and Bleakney, W., "The Attenuation of Spherical Shock Waves in Air," J. App. Physics 19, 670-678 (July 1948)

9. Kirkwood, J. G., and Brinkley, S. R., Jr., Theoretical Blast-Wave Curves for Cast TNT, National Defense Research Committee report No. OSRD-5481, August 23, 1945

10. Report of the Technical Director, Operation CROSSROADS, Vol I, Report No. XR-156, (Encl C), May 1947; Hartmann, G. K., et al, Blast Measurement Summary Report, Scientific Director's report on Operation SANDSTONE, Annex 5, Part I (SANDSTONE report No. 20), 1948

11. Porzel, F. B., and Reines, F., Height of Burst for Atomic Bombs, Los Alamos Scientific Laboratory report No. LA-743R, August 3, 1949

12. Pelsor, G. T., Overpressures Expected from an A-Bomb over a Rigid Plane, Sandia Laboratory report No. SC-1516(TR), July 19, 1950

13. Smith, L. G., Photographic Investigation of the Reflection of Plane Shocks in Air, National Defense Research Committee report No. OSRD-6271, November 1, 1945

14. An Analysis of the Strategic Uses of the Air-Burst Atomic Bomb with Special Reference to the Fuzing Problem, Sandia Corporation report No. SC-1827(TR), May 24, 1951

15. Hartmann, G. K., et al, Blast -- Measurement of Peak Pressure, Scientific Director's report on Operation SANDSTONE, Annex 5, Part II, 1948

16. Pressure-Time Measurements in the Mach Region, Scientific Director's report on Operation GREENHOUSE, Annex 1.6, Part IV

LIST OF REFERENCES (cont)

(GREENHOUSE report No. WT-53), July 1951; Northrop, P. A., Instrumentation of Structures Program, Scientific Director's report on Operation GREENHOUSE, Annex 3.4, Part II (GREENHOUSE report No. WT-10), August 1951

17. Murphey, B. F., Air Overpressure vs Time vs Distance for BUSTER Airburst Bombs, BUSTER-JANGLE report No. WT-304, March 4, 1952; Harding, J. M., Variation of Blast Pressures at Fixed Distances with Small Altitudes, BUSTER-JANGLE report No. WT-305, April 3, 1952

18. Supplement 1 to TM 23-200, Capabilities of Atomic Weapons, July 1951 (prepared for the Armed Forces Special Weapons Project by the Los Alamos Scientific Laboratory)

19. Murphey, B. F., Air Shock Pressure-Time vs Distance, TUMBLER-SNAPPER report No. WT-501, August 1, 1952

20. Operation TUMBLER Preliminary Report (prepared by the Armed Forces Special Weapons Project), TC-52-190D, Parts 1 and 2, May 15, 1952

21. Howard, W. J., and Jones, R. D., Free Air Pressure Measurements for Operation JANGLE by Project 1.4, Sandia Corporation report SC-2261(TR), February 19, 1952 (also published as WT-306, an integral part of WT-367)

22. Aronson, C. J., et al, Free Air and Ground-Level Pressure Measurements, TUMBLER-SNAPPER report No. WT-513, November 1952.

23. Murphey, B. F., Pressure-Distance-Height Data for 250-lb HE Spheres, preliminary report on Project 1.10 of Operation TUMBLER, Sandia Corporation memorandum 5111(65), March 13, 1952 (also published by AFSWP as a preliminary report on Operation TUMBLER, Annex VIII, under the same title)

24. Preliminary Experiments to Determine the Effect of Air Movement on the Pressure-Time Curves Given by Piezo-Electric Blast Pressure Gauges, Road Research Laboratory (Br) note No.

LIST OF REFERENCES (cont)

ARP/31/HS, April 1940; MacDonald, J. K. L., and Schaaf, S. A., On the Estimation of Perturbations Due to Flow Around Blast Gauges, National Defense Research Committee report No. OSRD 5639, September 1945; Schaaf, S. A., Estimates of Perturbations Due to Flow Around Blast Gauges with Spheroidal Shapes, New York University report No. AMG-NYU-144, 1946; Armstrong, A. H., and Hicks, E. P., The Aerodynamic Calibration of Blast Pressure Gauges, Ministry of Supply (Br) Armament Research Establishment report No. 34/54, February 1951

25. Marks, S. T., Response of Air Blast Gauges of Various Shapes as a Function of Pressure Level, Ballistic Research Laboratory report No. 734, August 1950 (see also reference cited in this report)

26. HE-Tests -- Operation JANGLE, Stanford Research Institute interim report, October 1951; Underground Explosion Tests at Dugway, Stanford Research Institute interim report, July 1951

27. Salmon, V. (Stanford Research Institute), Air Pressure vs Time, TUMBLER report WT-512 (to be published)

28. Shreve, J. D., Jr., Orientation of Gauge Baffles in Overpressure Measurements (special Sandia Corporation letter), ref sym 5111(68), September 2, 1952

29. Fisher, E. M., Air Blast Measurements on Spherical Cast TNT Charges, Naval Ordnance Laboratory report NOLM-10780, January 1950

30. Weibull, W., Explosion of Spherical Charges in Air: Travel Time, Velocity of Front and Duration of Shock Waves (translated from the original Swedish paper), Ballistic Research Laboratories Translation Report X-127, February 1950

31. Hartmann, G. K., et al, Blast Measurements -- Part I, Summary Report, Scientific Director's report on Operation GREENHOUSE, Annex 1.6, Part I (GREENHOUSE report WT-64), May 1952

LIST OF REFERENCES (cont)

32. Fisher, E. M., Experimental Shock Wave Reflection Studies with Several Different Reflecting Surfaces, Naval Ordnance Laboratory report Navord 2123, September 25, 1951

33. Stevens, Maj. G., The Behavior of the Shock Wave in Air from Small Underground Explosives, Naval Ordnance Laboratory report Navord 1863, April 26, 1951

34. Sachs, R. G., The Dependence of Blast on Ambient Pressure and Temperature, Ballistic Research Laboratory report 466, May 15, 1944

35. Dewey, J., and Sperrazza, J., The Effect of Atmospheric Pressure and Temperature on Air Shock, Ballistic Research Laboratory report BRL-721, May 1950

36. Curtis, W., Free Air Blast Measurements on Spherical Pentolite, Ballistic Research Laboratory memorandum report 544, July 1951

37. Hartmann, G. K., and Kalavski, P. Z., The Optimum Height of Burst for High Explosives, Naval Ordnance Laboratory report Navord 2451, July 21, 1952

38. Arons, A. B., and Tait, C. W., Design and Use of Tourmaline Gauges for Piezo-Electric Measurement of Air Blast, National Defense Research Committee report OSRD-6250, 1946

39. Merritt, M. L., Effects of Surface Roughness on Blast Waves, Sandia Corporation report SC-1604(TR), October 30, 1950; Eberhard, R. A., et al, Effect of Solid Walls on the Mach Region, Ballistic Research Laboratory report 759, May 1951

40. Duff, R. E., "The Interaction of Plane Shock Waves and Rough Surfaces," J. App. Physics 23 (12) 1373-9 (1952)

41. Bryant, E. J., et al, Mach Reflection over Hard-Packed Dirt and Dry Sand, Ballistic Research Laboratory report 809, July 1952

LIST OF REFERENCES (cont)

42. Porzel, F. B., Height of Burst for Atomic Bombs, Los Alamos Scientific Laboratory report LA-1406 (to be published)

43. Eberhard, R. A., et al, Peak Air Blast Pressures from Shock Velocity Measurements along the Ground, Operation JANGLE report WT-323 (no date) (published as an integral part of Operation JANGLE report WT-366)

APPENDIX A

THE 20-KC CARRIER SYSTEM

by R. O. Ferner, Sandia Corporation

In the pressure-recording system used for this study a 20-kc carrier signal is fed to a Wiancko air pressure gauge, which modulates the carrier to a degree determined by the impressed air pressure. The modulated signal is in turn rectified, filtered free of the 20-kc carrier signal, and fed to a high-frequency string galvanometer in a standard Consolidated Engineering Corporation oscillographic recorder, which makes a permanent pressure-time record in the usual fashion. The system merits description here by virtue of its high frequency response as compared with standard Consolidated auxiliary equipment (System D). Specifically the system developed at Sandia Laboratory has an over-all frequency response of 0-3000 cps and a range of 1-800 psi. Refinements to the basic system have been dictated by a desire to improve signal-to-noise ratio, linearity, frequency response, and dynamic recording of the calibration signal. Such practical considerations as expense, availability of materials, and convenience of operation have also played a significant role in the final design of the system.

The block diagram (Fig. A.1) will serve as a guide in describing the operation of the system. A master driver consisting of a 20-kc oscillator-amplifier feeds one secondary amplifier for each set of nine gauges. This secondary amplifier feeds a 20-kc carrier signal from its 600-ohm balanced output over 1000 feet of Twinax cable to a distribution station, which is merely an impedance-matching transformer to terminate the 600-ohm line and feed the nine gauges in parallel from an 8-ohm secondary winding. From a small distribution panel at the distribution station a separate 3-conductor shielded cable runs to each gauge. Two of the conductors transport the 20-kc carrier to the gauge. A resistance network mounted on each gauge reduces interaction between gauges through the common carrier source and increases the phase stability of the carrier signal by damping any resonances. At the center tap of the gauge there appears a 20-kc signal whose amplitude is proportional to the air pressure sensed by the

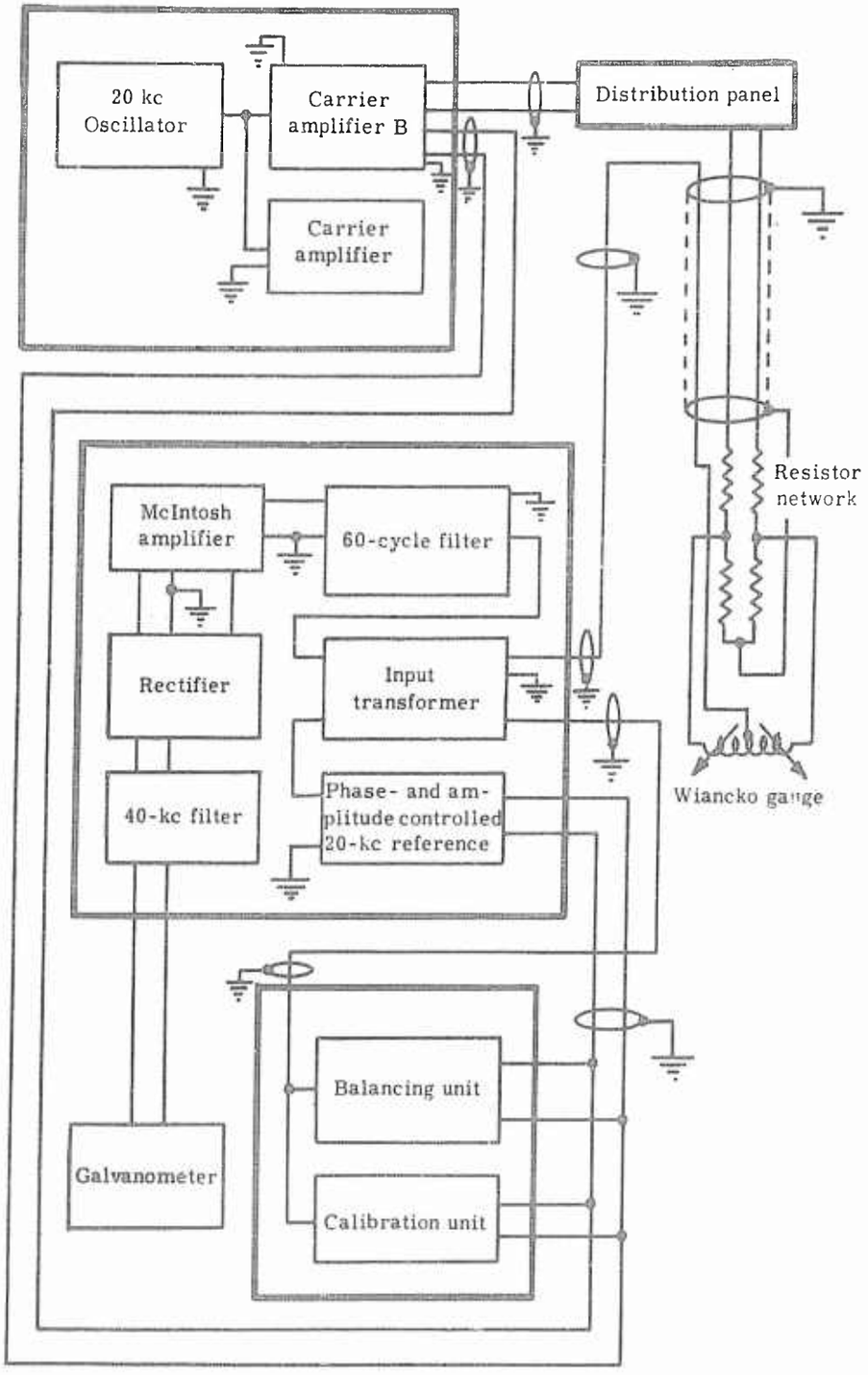

Fig. A.1. -- Diagram of the Recording System

gauge; this modulated carrier signal returns by way of the third conductor to the distribution panel and from there is transmitted to the receiver over 1000 feet of coaxial cable.

Nine receivers (Fig. A.2) are arranged on a standard panel rack (Fig. A.3) which also holds a calibration unit that feeds all receivers. The input signal to the receiver is fed into one side of a balanced line-to-grid transformer (Fig. A.4), the other side of which may receive a signal from the calibration unit. As shown in Figs. A.1 and A.4 the secondary of this transformer is coupled to the amplifier of the receiver through an R-C filter designed to attenuate accumulated 60-cps pickup. The other side of the secondary is connected to the phase and amplitude control circuit of the receiver, which supplies a 20-kc reference signal in phase with the modulated 20-kc signal from the gauge. The amplified composite 20-kc signal is fed from the 600-ohm balanced out-put to a full-wave rectifier consisting of two G-10-C germanium diodes having extremely low forward resistances. The rectified output passes in sequence through a 3-kc low-pass L-C filter, (40-kc filter of Fig. A.1), a reversing switch, and a monitoring 50-0-50 d-c milliammeter to the galvanometer string.

The 20-kc reference signal manifests itself as a d-c bias on the galvanometer string, and the intelligence is superimposed on this bias. The bias ensures that the rectifiers will operate in a linear region and that a negative pressure on the gauge will be accurately recorded as a decrease in bias level. Figure A.5 illustrates this effect. When no bias is applied (Fig. A.5a), the negative phase (cross-hatched portion) is inverted, and all portions of the signal near the zero level are distorted since this in a nonlinear region of rectifier operation. Figure A.5b shows that an accurate pressure signal results through the use of sufficient bias.

Before the system can be used for actual pressure measurements a number of adjustments are necessary. It is important that the frequency response of each receiver-galvanometer combination be ascertained. A 20-kc carrier, modulated by a 1-kc square wave, is introduced at the input to the receiver and the inductance of the 3-kc low-pass filter in the receiver unit varied until the galvanometer string reproduces the 1-kc square wave with an overshoot of about 2 per cent. Once this adjustment is made the receiver and galvanometer are considered matched and are always used together. The gauges are connected as shown in Fig. A.1. Since they are not perfectly balanced and since there is always some stray pickup in the

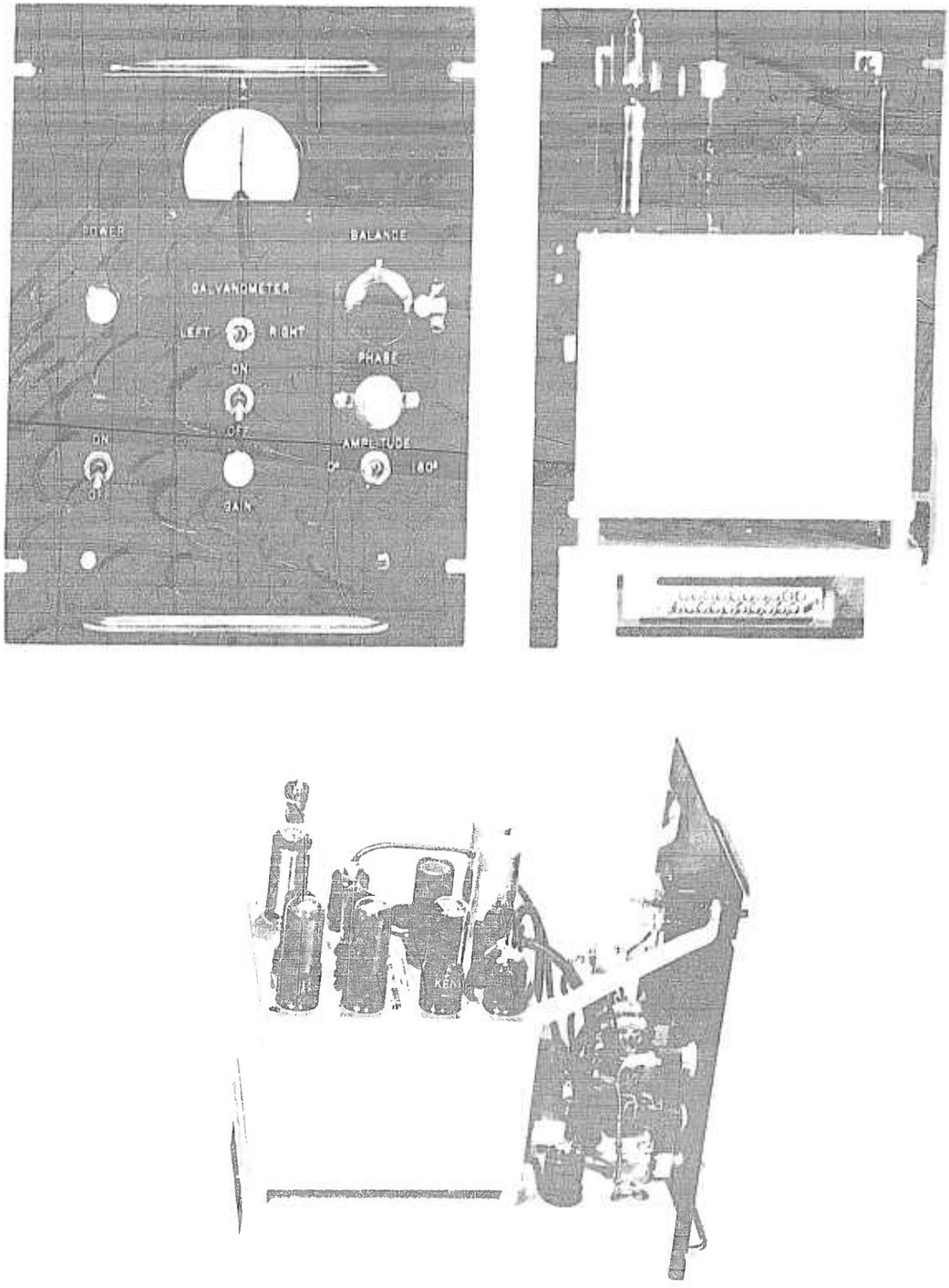
POWER
BALANCE
GALVANOMETER
LEFT
RIGHT
ON
OFF
PHASE
AMPLITUDE
0°
180°
ON
OFF
GAIN

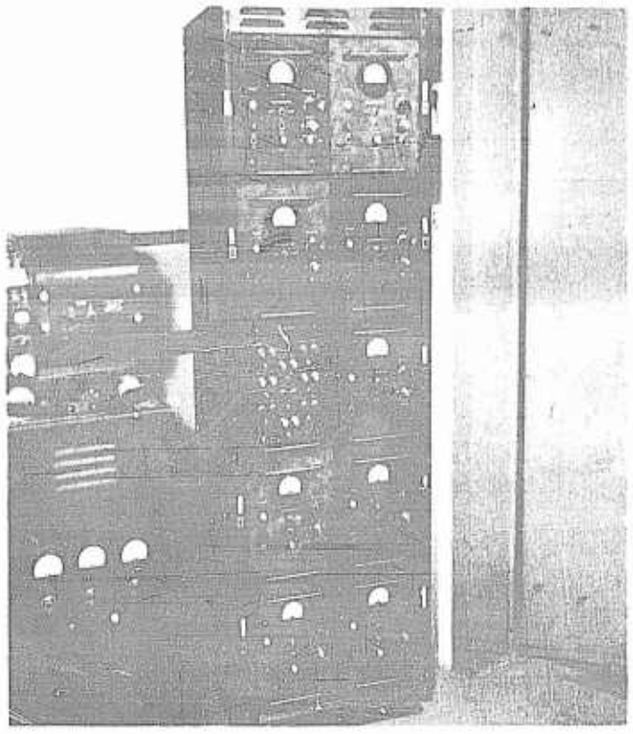

Fig. A.3. -- Standard Receiver Rack

3-conductor cable, a 20-kc signal appears at the input to each receiver. This background signal is reduced to zero or to a minimum by adjusting the phase and amplitude controls of the calibration unit to introduce a signal equal and opposite in phase. Any harmonic content of the 20-kc background can not be balanced out and may appear as a small residual deflection of the meter. Completion of these adjustments readies the system for calibration.

A static pressure equal to the expected peak transient pressure is now applied at the gauge and the gain of the receiver adjusted sc that the pressure signal produces an output of about 25 milliamperes. Next the amplitude control of the receiver is advanced to obtain an additional signal from the 20-kc reference phase, after which the phase control is adjusted to produce a maximum deflection on the meter and ensure that the bias signal is exactly in phase with the pressure signal. Since the phase control has a range of only 170^{o}, the phase should be adjusted for both positions of the reversing switch to make certain that the best maximum reading is obtained. The static pressure on the gauge is then released, and finally the bias is adjusted by means of the amplitude control to give a signal of about 10 milliamperes.

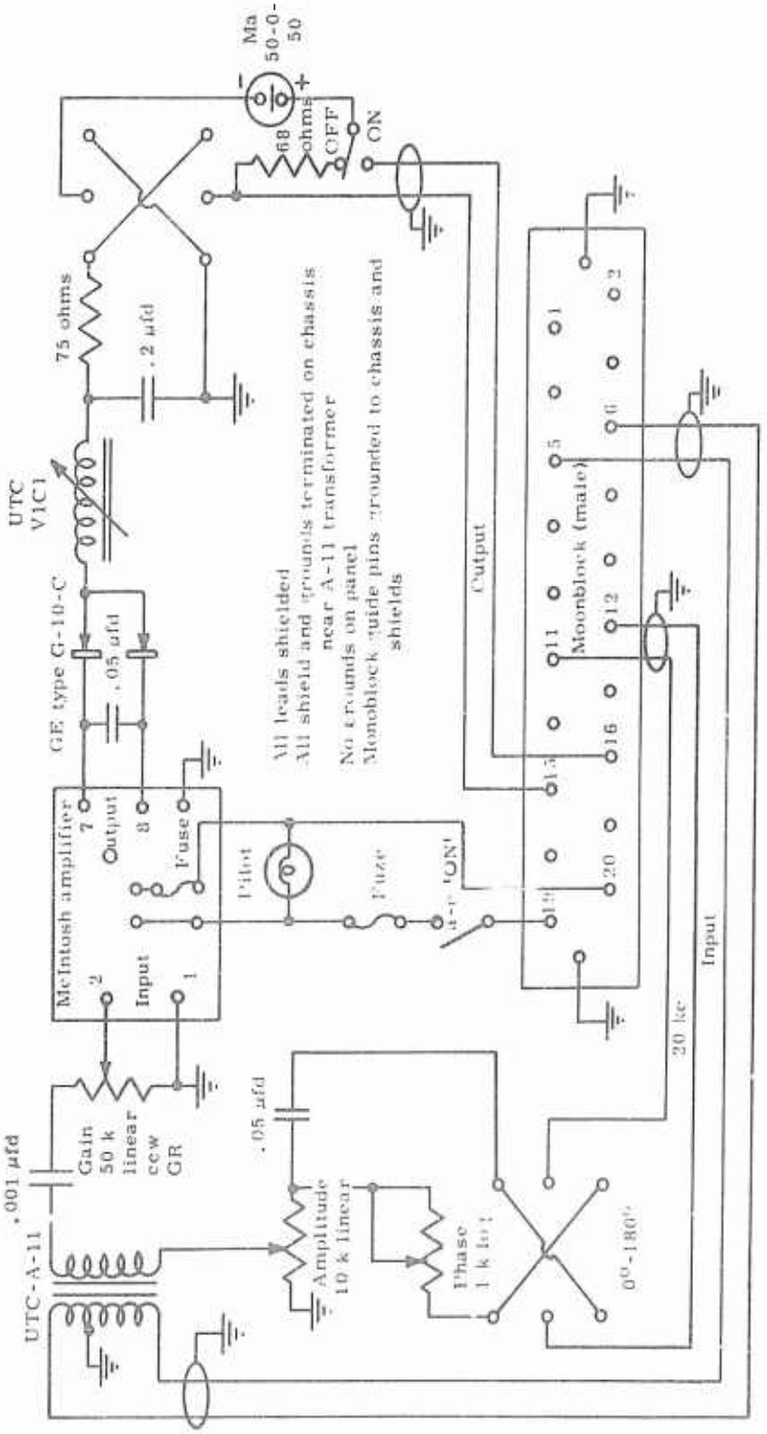

Fig. A.4. -- Schematic Diagram of the Receiver

A. 5a

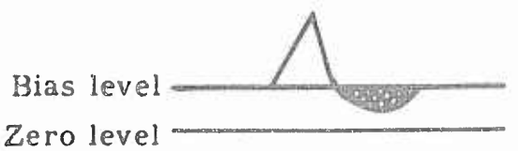

A. 5b

Fig. A. 5. -- Effect of Impressing a Bias on the Recorded Signal

It is important to understand that static calibration of the recording system is a time-consuming procedure and that some time is also required to assemble the TNT hemispheres, place the detonator, and raise the charge into position for firing. Thus an interval of 1-3 hours elapses between calibration of the first gauge and firing time. Any drift of the system during this period would add uncertainty to the precision of the pressure measurements.

To minimize this uncertainty a dynamic check of the system is performed by means of the calibration unit (Figs. A. 6 and A. 7). Capacitances and resistances can be chosen which will make it possible to produce a galvanometer deflection equal in phase and magnitude to that produced by applying a known static pressure to the gauge. One such capacitor-resistor combination* is fabricated for each set range of a particular gauge. By means of a relay this simulated pressure signal can be applied either automatically or manually to the input of each receiver and removed immediately before the pressure signal is received from the gauge. This calibration signal is repeated

*For the particular gauges used in this study it was found that capacitors alone gave the desired simulated pressure signal.

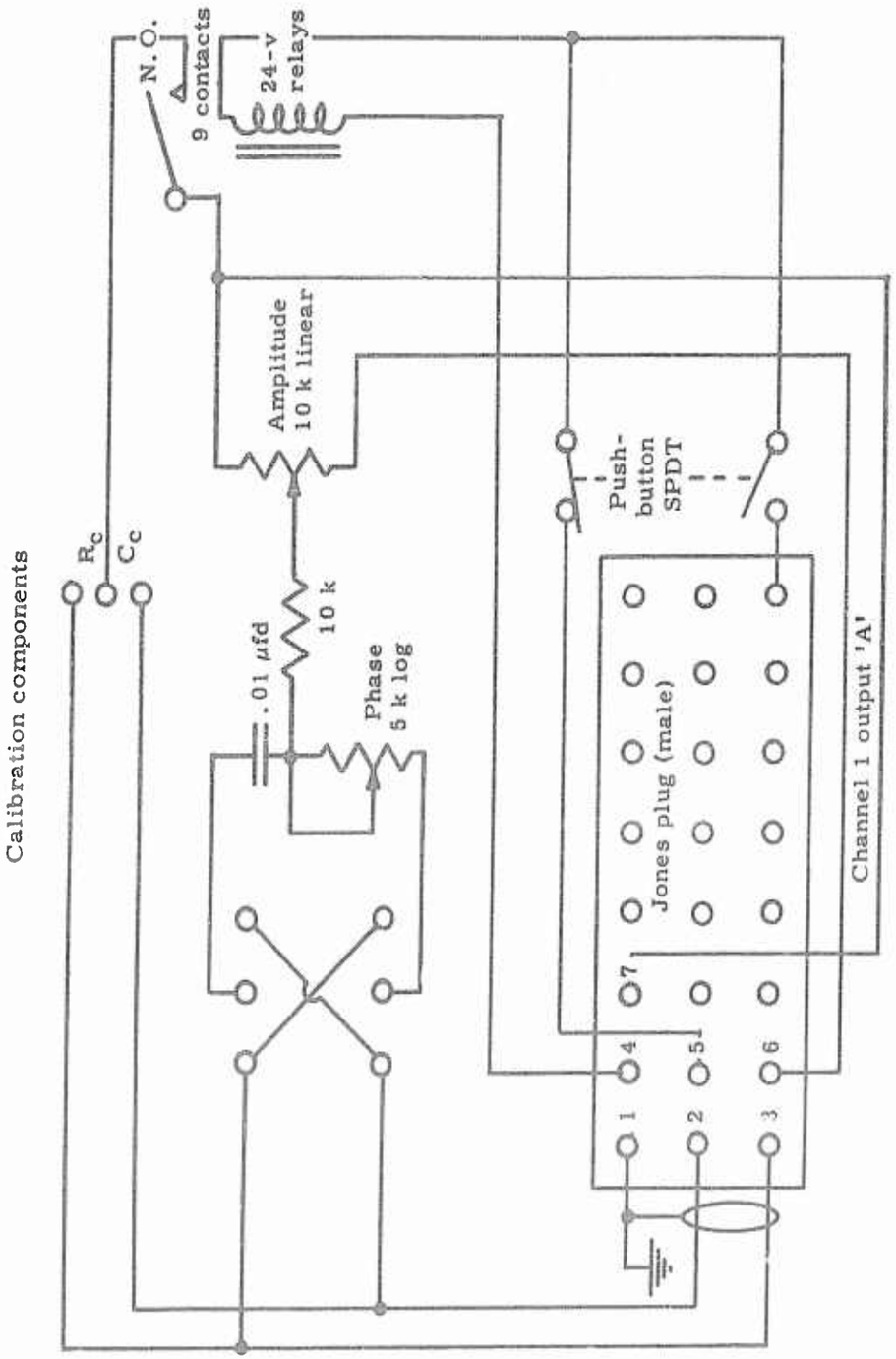

Fig. A.6. -- Schematic Diagram of the Calibration Unit

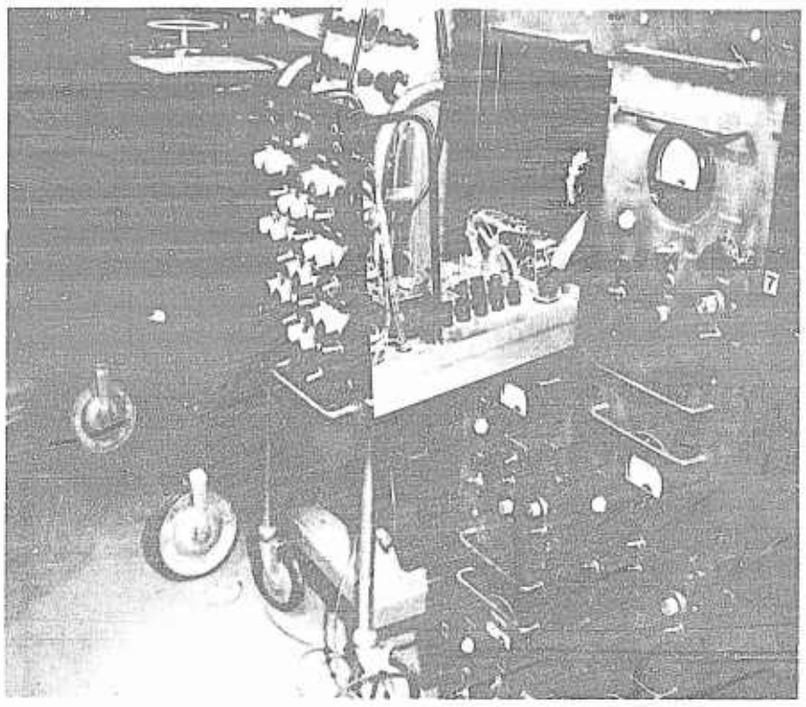

Fig. A.7. -- Calibration Unit

immediately after the pressure intelligence is recorded. Thus the system is effectively recalibrated within a fraction of a second before and and after the gauge is used to measure the desired intelligence. As mentioned previously, one calibration unit serves nine information channels.

The frequency response of the system in operation seems to depend upon the type of gauge used. Rise times of the order of 0.15 millisecond were obtained using the latest type of Wiancko air pressure gauge.

Determination of rise time is made by applying a shock from a small shock tube to the gauge in position and recording the output of the receiver on an oscilloscope.*

*A detailed discussion of gauge characteristics, damping procedures, and adjustments to the gauges appears as Appendix B.

The over-all accuracy of the system is believed to be greater than 5 per cent. The correspondence of static pressure and the simulated pressure signal is checked daily and has been found to vary by less than 2 per cent for the majority of the gauges although for several it was found to vary by as much as 5 per cent.

Steps have been taken to correct difficulties arising from leakage paths caused by moisture condensation at the gauges, dirt from the blast entering the bourdon tubes, and faulty connections arising from constant handling of the gauges.

APPENDIX B

THE WIANCKO AIR-PRESSURE GAUGE

by E. J. Vulgan, Sandia Corporation

Changing weather conditions at the Coyote Canyon test site placed significant restrictions upon the electrical and mechanical characteristics of the gauge to be used in this series of measurements. The gauge had to be insensitive to the effects of extremes in heat and cold, electrical and dust storms, and heavy rains. Notable diurnal and seasonal variations in atmospheric static discharge were observed. It was also found that the soil in the area, when dry, acted as an excellent electrical insulator, whereas addition of even small amounts of moisture caused it to become a conductor.

These factors, coupled with requirements imposed by the experiment, resulted in comparatively rigid specifications for electrical and mechanical characteristics of the gauge. The desired time resolution of the gauge system and the magnitudes of the pressures to be measured by individual gauges determined optimum combinations of pressure sensitivity and frequency response; in the interest of accuracy and reproducibility of results it was imperative that nonlinearity of response, temperature effects, and any error introduced by hysteresis be minimized; finally, it was desired that the sensing area of the gauging element be as small as possible, that the gauge have the requisite accuracy, and that it be insensitive to sustained vibration and acceleration.

Following tests of numerous gauges of several types it was found that the variable-reluctance bourdon-type gauge manufactured by the Wiancko Engineering Company best met specifications. Futhermore, this gauge was available in sufficient quantity to instrument the proposed experiment. Two models of the gauge, the 3PAD and the 20PAD-WS (Figs. B.1 and B.2), were used; they are identical in principle of operation but differ in the lengths of the bourdon tubes, the inductances of the E-coils, and the type of bleed arrangement used in the back volume or reference chamber of the gauge.

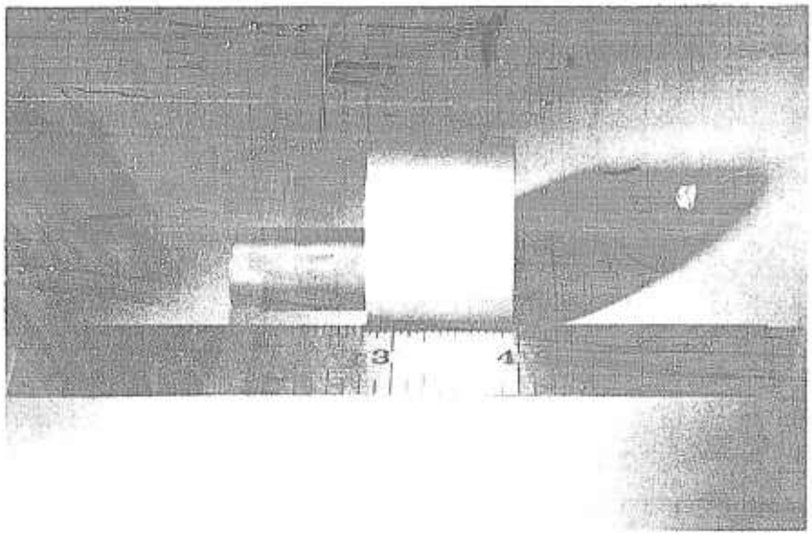

Fig. B.1 -- 3PAD Gauge

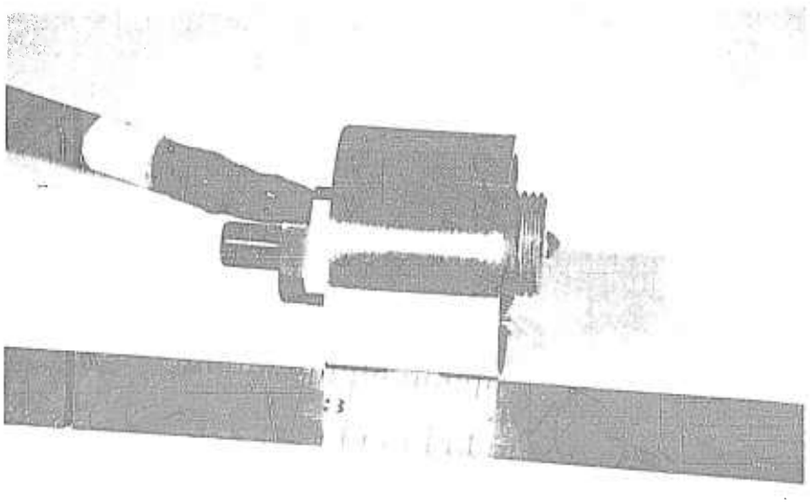

Fig. B.2. -- 20PAD-WS Gauge

The sensing element of the Wiancko gauge* is a flat twisted bourdon tube (Fig. B.3) whose open end is fastened securely to the frame of the gauge. Unlike the usual form of the bourdon tube, which straightens in response to an internal pressure, the twisted tube acts in torsion, imparting a rotation to a vane attached to the sealed end. This vane forms the armature of a variable-reluctance system comprised of an E-core and two E-coils (Fig. B.4). Mechanical angular displacement of the armature changes the reluctance of the two magnetic loops of the E-core and results in the modulation of the carrier current flowing through the E-coils. Variations in applied pressure are thus translated into electrical signals which are in turn amplified and recorded.

At the start of this series of tests the Model 3PAD gauge was the only Wiancko gauge of this type available. Its total inductance is 40 mh, and its bourdon tube is 1.6 inches long. It was found, however, that the frequency response of this model was not adequate, particularly in the lower-pressure regions, to obtain the high-frequency intelligence needed in certain phases of the program. The manufacturer was therefore approached and found willing to modify the 3PAD gauge to meet requirements for quicker response. The result was the 20PAD-WS gauge; its significant features are a bourdon tube only 0.65 inch long (Fig. B.2) and E-coils having a total inductance of only 7.5 mh. The lesser inductance, it was believed, would be more compatible with the desired high-frequency carrier, which has a frequency of 20 kc as compared with the 3 kc normally used with the older gauge system.

The reference chambers of both models of the gauge are equipped with bleed arrangements to permit automatic adjustment to slow changes in ambient or barometric pressure. An innovation in the 20PAD-WS gauge is the variable and removable bleed plug that makes the same gauge usable either as an overpressure or differential pressure measuring instrument. The original 3PAD model had a porous plug type bleed and could be transformed into a differential pressure measuring gauge only after modification. However, the manufacturer is currently taking steps to incorporate the variable bleed into the 3PAD gauge.

---

*Earlier models of the Wiancko gauge are described in WT-1, Instrumentation for Structures Program, Scientific Director's report on Operation GREENHOUSE, Annex 3.4, Part 1, January 1951, by P.A. Northrop (Confidential).

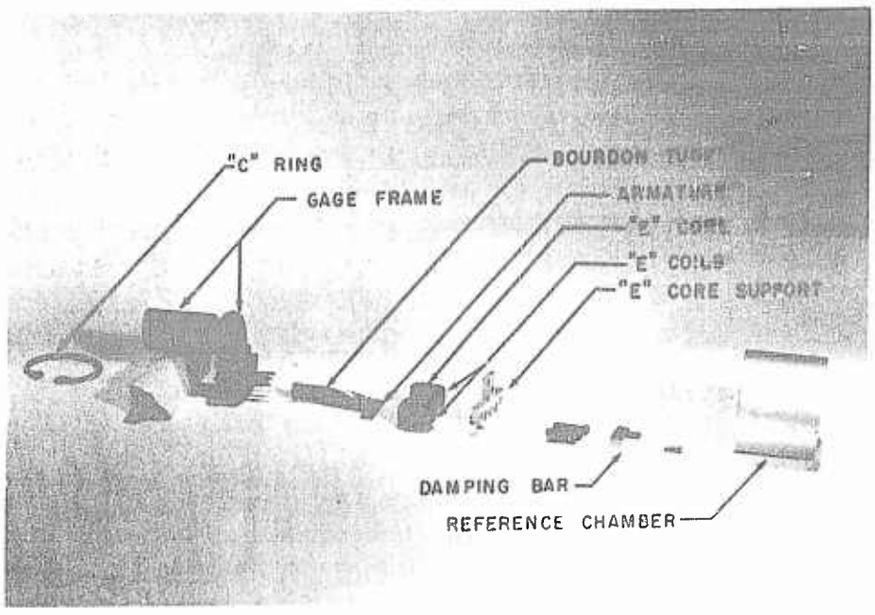

Fig. B.3 -- Exploded View of the 3PAD Gauge

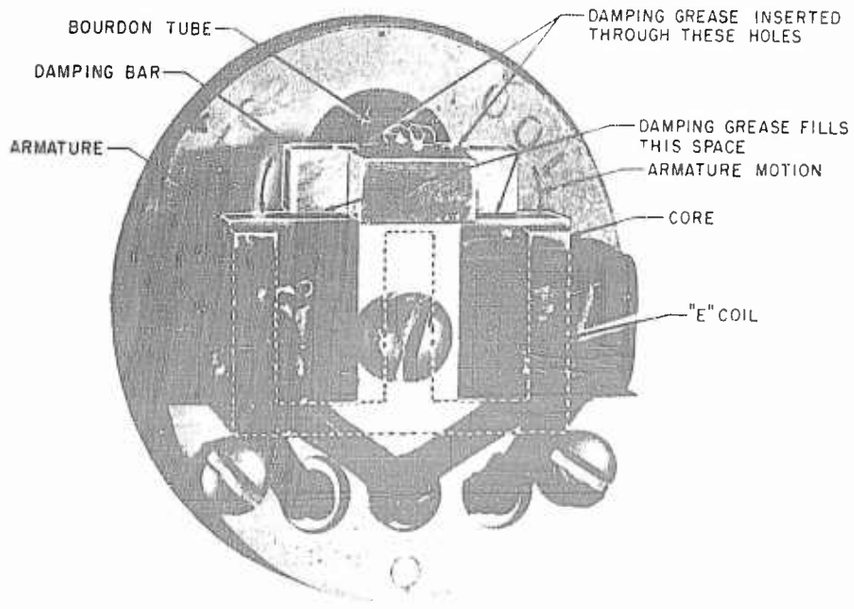

Fig. B.4 -- End View of the 3PAD Gauge

Before these gauges can be used in the field, they must be damped acoustically as well as mechanically. Since the open end of the bourdon tube, in use, faces into the pressure transient, it is easily excited to acoustical resonance at a frequency which is a simple function of the length of the tube. It is interesting to note that the experimentally determined acoustic resonant frequencies were within 20 cps of the resonant point calculated by assuming the bourdon tube to be a simple quarter-wave, closed-end pipe. The bourdon tube of the 3PAD gauge resonates at about 2 kc, whereas that of the 20PAD-WS gauge resonates at about 5 kc. The resonant frequency is excited by passing a stream of air across the opening of a gauge which has not been acoustically damped. The resultant whistle is picked up by an adjacent microphone, fed through an amplifier, and viewed on a dual-beam oscilloscope simultaneously with the output of a standard audio oscillator. The two traces are matched, and the frequency of the whistle is read on the calibrated dial of the oscillator.

Fortunately signals caused by acoustic resonance can be virtually eliminated by careful insertion of a wick of spun glass braid into the bourdon tube in sufficient quantity to fill the tube but not deform nor offer resistance to its movement. Acoustic damping is completed prior to mechanical damping so that the mechanical ringing can be seen clearly during the ensuing mechanical damping procedure. Adequacy of acoustic damping is determined by subjecting the gauge to a pressure step in a specially constructed shock tube* and photographing the electrical output of the gauge as recorded on an oscilloscope screen. Insufficient acoustic damping is evidenced by a high-frequency ring at the peak of the pressure pulse, superimposed on the lower-frequency ring of the mechanical system. Knowing the frequency of acoustic resonance permits discrimination between the two signals even for the higher-pressure gauges. Figures B.5a, b, c trace stepwise the gauge response from the completely undamped state to proper damping under laboratory conditions. Figure B.5d has been added to indicate the effect of acoustic ringing alone.

Mechanical resonances of the gauges were determined by two methods; undamped gauges were either submitted to variable-frequency

*This shock tube is described by W.J. Howard and R. D. Jones in Sandia Corporation report SC-2261(TR), Free Air Pressure Measurements for Operation JANGLE by Project 1.4, February 19, 1952. This report has also been published as the final chapter of WT-367, Blast and Shock Measurements II (no date) (Secret).

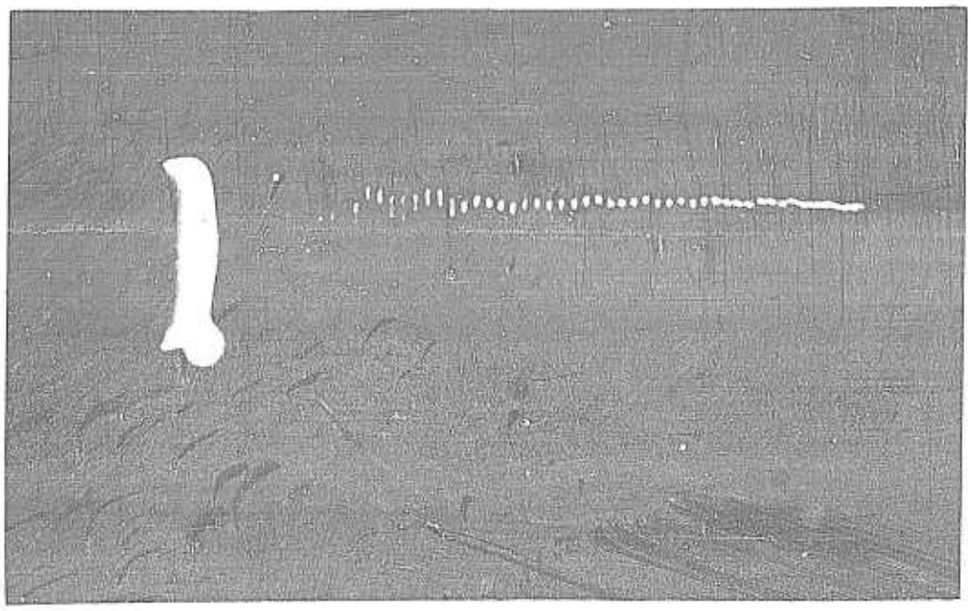

Fig. B. 5a -- Oscilloscope Record of an Undamped Gauge

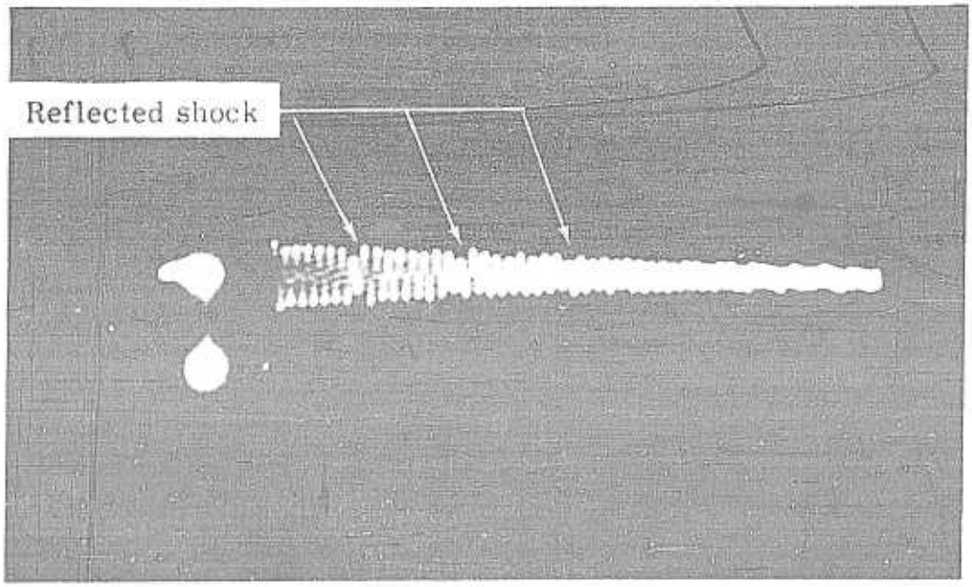

Fig. B. 5b -- Oscilloscope Record of a Gauge Having Acoustical Damping Only

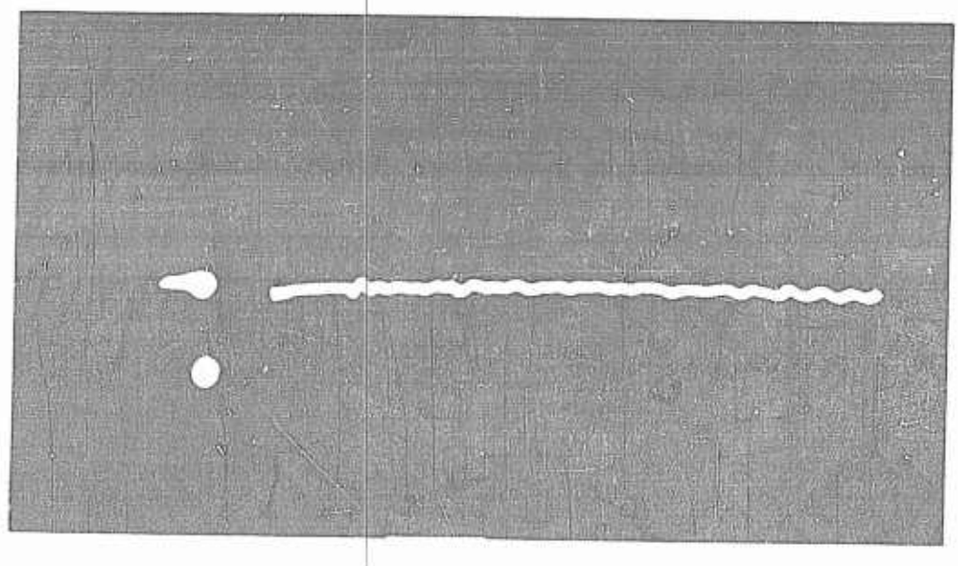

Fig. B.5c -- Oscilloscope Record of a Properly Damped Gauge (Acoustical and Mechanical Damping)

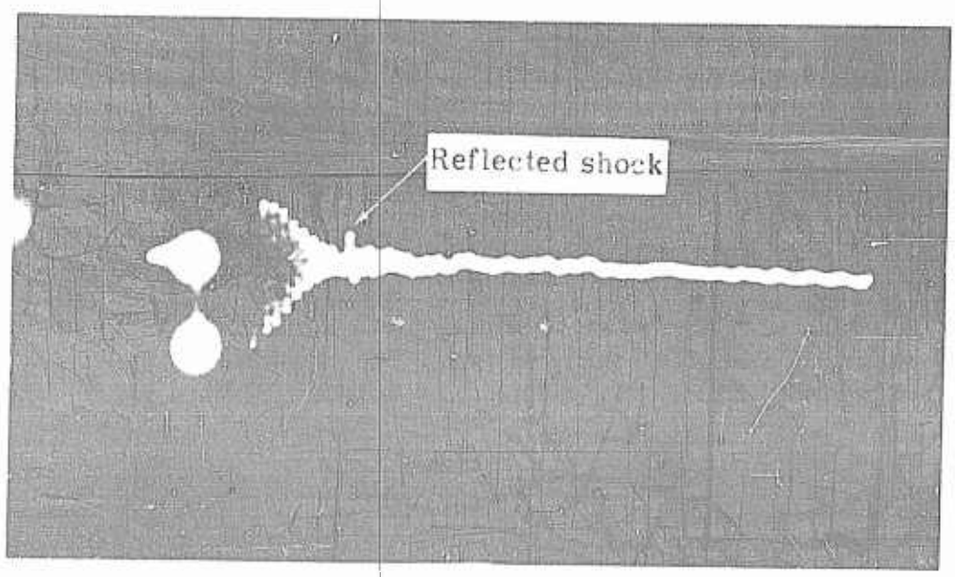

Fig. B.5d -- Oscilloscope Record of Gauge Having Mechanical Damping Only

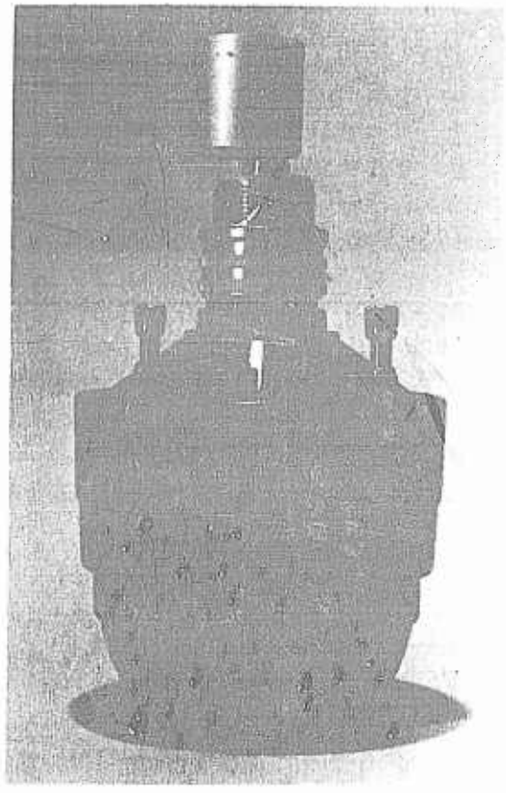

Fig. B.6 -- Audio Driver Unit

vibration of the order of 0.75 g in a Calidyne shaker or driven by means of an air column from an audio driver unit (Fig. B.6). Results of the two methods of test were essentially identical. At mechanical resonance a large-amplitude signal is observed. The resonant peak is of the order of 100 cycles wide. Table B.1 lists observed mechanical resonant frequencies for several gauges; actual resonant frequencies of all gauges used within a given pressure range vary by no more than 100 cps from the frequencies listed here.

It will be noted that the mechanical resonance of the 50-pound 20PAD-WS gauge used here is only 100 cps higher than that for the 50-pound 3PAD gauge; however, the higher frequency of acoustic resonance makes the 20PAD-WS type gauge superior. Later models of the 20PAD-WS 50-pound gauge having a resonant frequency of 3600 cps are available.

TABLE B.1

Observed mechanical resonant frequencies
for various 3PAD and 20PAD-WS gauges

Serial No.	Pressure range (psig)	Mechanical resonant frequency (cps)
Model 3PAD (long bourdon tube)		
5002	10	1625
1981	30	1950
1885	50	2400
2035	100	2570
6100	200	3600
7708	500	3800

TABLE B.1 (cont)

Serial No.	Pressure range (psig)	Mechanical resonant frequency (cps)
Model 20PAD-WS (short bourdon tube)		
11112	10	2100
8623	50	2500
8621	100	4400
8614	500	6300

The mechanical system of the gauge is damped by placing a Dow-Corning silicone grease, DC-4*, between the damping bar and armature of the gauge (Fig. B.4), using a medicinal hypodermic syringe. If too much grease is inserted, it may be removed by using narrow strips of paper. Response of the gauge, in the shock tube, to a pressure step having a rise time of 10 microseconds is also used as a check of effectiveness of mechanical damping. When experimental attempts were made to overdamp the gauge as originally received from the manufacturer, its resonant frequency, instead of decreasing as was expected, actually increased. Careful analysis revealed that the damping bar itself oscillated; the energy to initiate this oscillation apparently was transmitted through the damping grease. Increasing the thickness of the damping bar eliminated this spurious oscillation.

Pressure-time records from shock-tube tests of some of the gauges evidenced a slowing down of the measured pressure pulse before it reached its peak value (Fig. B.7a); apparently the action of

*Manufactured primarily for high-voltage insulation purposes; mixtures of DC-4 and DC-7 have also been used satisfactorily for damping this gauge. Although different lots appear to vary slightly in viscosity, DC-4 grease is the most satisfactory of the numerous oils, greases, and other fluids tried. The temperature-viscosity coefficient, though significant, is considerably less for DC-4 than for other materials tried.

the gauge was impeded in some manner. This phenomenon, termed 'creep', is always observed within the first few milliseconds (0.5-4.0 milliseconds) of the rise time or peak pressure applied. An investigation of the response of the electrical system indicated creep to be inherent in the gauge itself and not in the electrical system. When the parameters affecting gauge response, particularly the damping media, were varied, results suggested several possible contributory factors, the most likely of which appeared to be hysteresis caused by an excess of damping grease and use of too narrow a gap between the damping bar and armature.

Present plans call for an investigation of grease hysteresis as it affects the damping of Wiancko gauges. It is likely that the width of the damping bar-armature gap may have a significant role in grease hysteresis since it has been found* that the viscosity of a lubricating oil increases rather sharply, often to that of a semisolid, at a distance of 0.15 to 2.0 microns from the solid surface, ie, at a depth of about 20-200 molecules. Every effort was made, in using the gauges, to maintain the ratio of creep to peak overpressure at a minimum consistent with adequate damping. In fact, the gauges were slightly underdamped in the laboratory to prevent the onset of creep with increased damping force at the lower temperatures encountered in the field (Fig. B.7b).

In the course of selecting the gauge to be used for these measurements a series of functional and environmental tests was conducted in the laboratory. As has been pointed out, pressure sensitivity and frequency response were found to be interdependent characteristics of the Wiancko gauge. Outputs of the 3PAD gauges were approximately 10 per cent of the carrier (supply) voltage for the maximum pressure ratings of the gauges; outputs of the 20PAD-WS gauges were about 8 per cent of the carrier voltage. The strong signal typical of Wiancko gauges is an extremely important feature for two reasons. A large signal-to-noise ratio can be maintained for long cable runs even in areas having normally high background levels of electrical noise. Moreover, the gauges can be used with confidence at a third or fourth of their nominal pressure ranges.

*Bondi, A., Physical Chemistry of Lubricating Oils, Reinhold, 1951, p 114

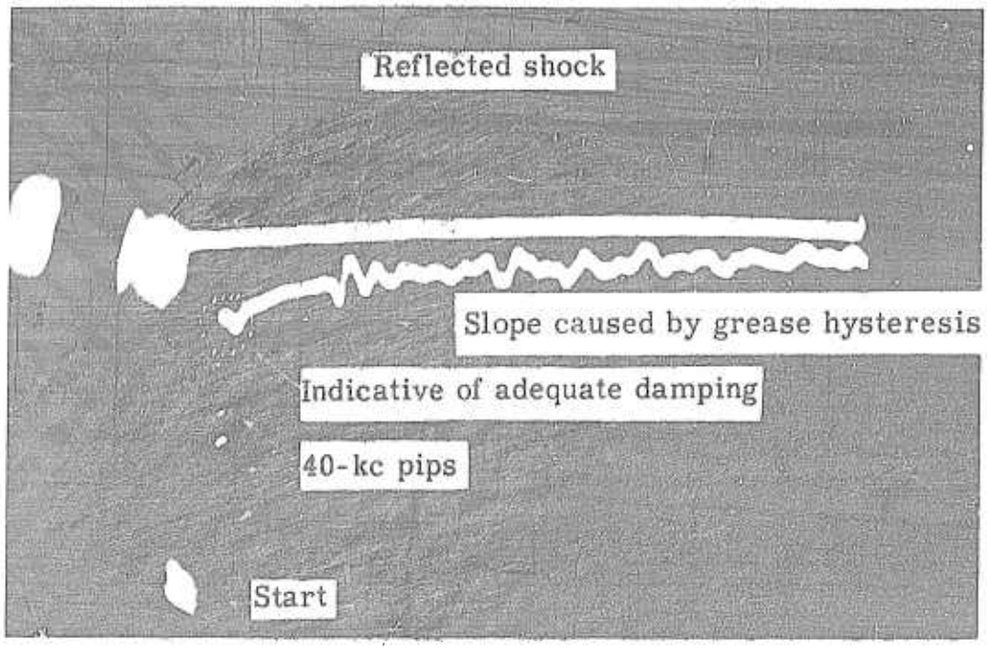

Fig. B.7a -- Oscilloscope Record of Gauge Exhibiting Creep. (This condition is that approached by a gauge that is well damped at room temperature upon use under winter field conditions.)

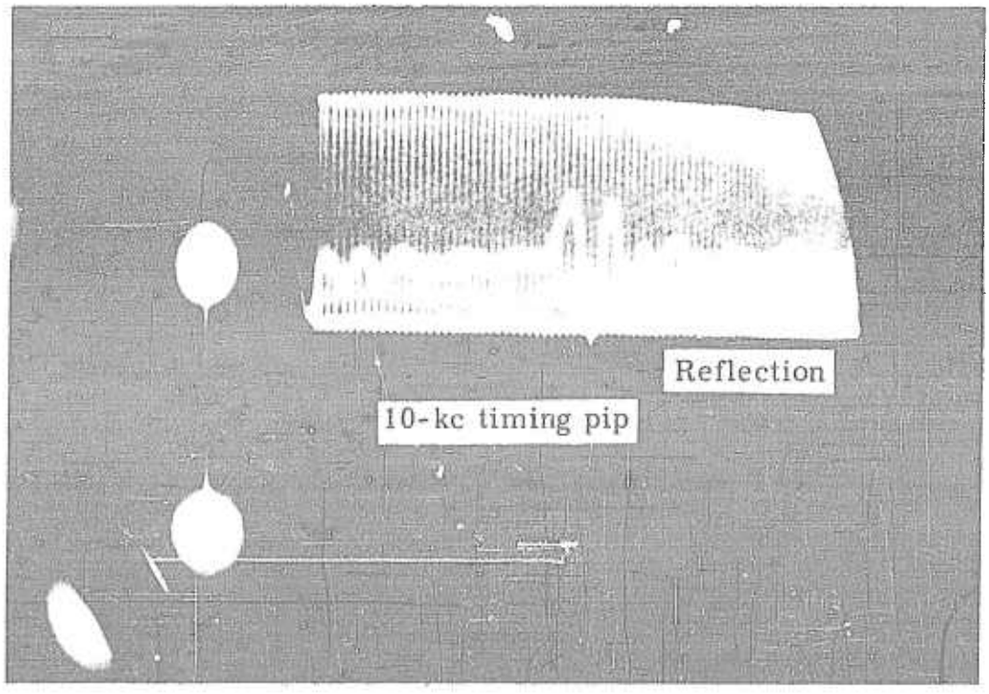

Fig. B.7b -- Oscilloscope Record of Gauge Purposely Underdamped. (Gauge underdamped to ensure satisfactory operation under winter field conditions. Record was made at room temperature.)

To determine whether the responses of these gauges were reasonably linear and whether any appreciable error in measuring small overpressures could result from hysteresis in the mechanical system of the gauge, a series of linearity and hysteresis tests was run on a representative group of gauges. The results of one such test on a 30-psi gauge are presented graphically in Fig. B.8. It was noted that regardless of the range of the gauge, 0.25 psi hysteresis was found.

The sensitivity of the gauge to different ambient temperatures was found to be of the order of 0.5 per cent of the pressure being measured over a range of 20° to 90°F.

To determine whether the Wiancko gauges were rugged enough to withstand vibrations and accelerations of the magnitudes anticipated in these tests they were subjected to shake table and drop tests in three directions: perpendicular and parallel to the plane of the armature and axial to the bourdon tube. When subjected to 50 g for 30 msec on the drop table a 10-pound gauge gave a response of 1/4 pound in two directions, that parallel to the plane of the armature and that axial to the bourdon tube. The 30-, 50-, and 100-pound gauges gave responses of 1/2 pound in the plane perpendicular to the plane of the armature, the most critical direction. There was no significant response when the gauges were accelerated at 300 g for 2 msec. It was felt that conditions of the acceleration tests were stringent enough to be indicative of inuse conditions. Next, a properly damped gauge was subjected to vibration tests on the Westinghouse shake table. No significant resonances were observed in the frequency range of 20-500 cps applied at accelerations as great as 20 g. It is regrettable that equipment was not available to make shake tests at higher frequencies.

The small size of the Wiancko gauge (Figs. B.1 and B.2) makes it eminently suitable for use on scaled blast studies; in fact, the orifice of the sensing element is small enough (3/8 inch nominal diameter) to make it suitable for in-use measuring side-on or varying stagnation pressures on the comparatively small surfaces of model structures. The possibility of placing these gauges very close together (a few inches center-to-center) also makes them useful in such applications as studying Mach stem and vortex formation.

In the gauges as received from the manufacturer the acoustic damping wick is inserted and cemented to the sealed end of the bourdon

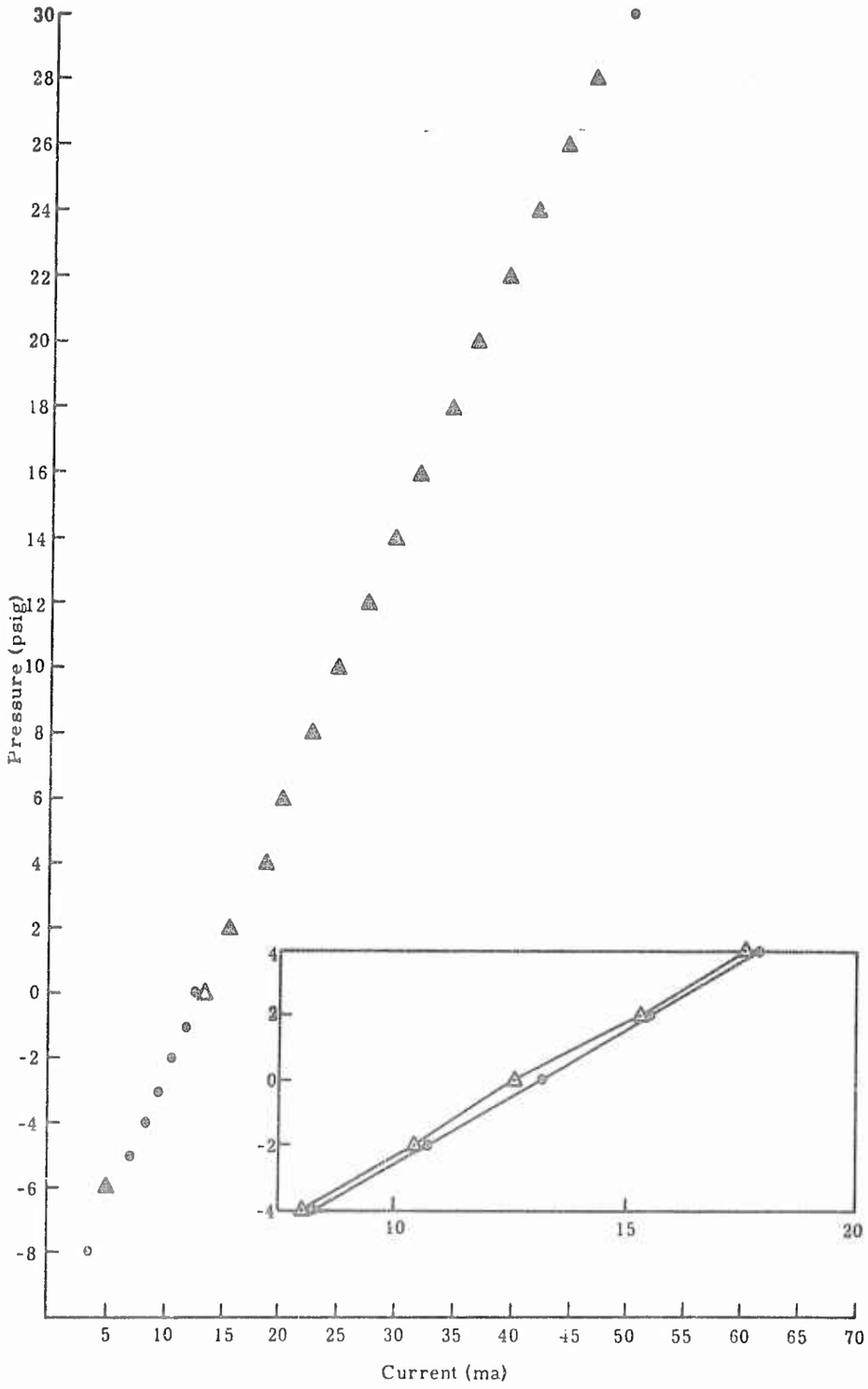

Fig. B. 8 -- Curve Illustrating Linearity of Response of a Typical Gauge

tube. The damping wick is a braid of sixteen strands of glass filaments, each strand of which comprises three bundles of filaments. Since the fill time of the bourdon tube is an important factor in determining the response of the gauge and will vary slightly from gauge to gauge, the quantity of damping wick needed will vary correspondingly. To compensate for this variation the thickness of the braid may be modified by removing as many as six strands of glass filaments.* The new wick is cemented into place, using the smallest possible quantity of latex cement; the cement is applied to the end of the wick that is to adhere to the bottom (sealed end) of the bourdon tube.

In early field tests using the Wiancko gauges difficulty was experienced with the connector cables breaking during frequent removal and reinstallation of the gauge canisters. Because it was necessary to screw the canister into the mount, the cables were subject to excessive twisting which caused them to break off at the solder joints within the connectors. A method was devised for installing the canister in the pipe cap gauge support without twisting it. The new method uses a threaded chamfered retaining ring and a beveled canister (Fig. B.9). A standard bronze canister modified in this fashion was used as the mount for the 3PAD gauge.

It was necessary to design a new type of mount† (Fig. B.10) for the 20PAD-WS gauge, primarily because of the change in the length of the bourdon tube and the resulting change in the design of the gauge frame on the part of the manufacturer. Rather than being threaded on the inside, as on the 3PAD gauge, the gauge frame of the 20PAD-WS gauge was threaded on the outside, necessitating a change in the method of attaching the hose fitting to the open end of the bourdon tube for static pressure calibration. A removable chamfered nut which fits flush with the outer face of the mounting disc and with the opening of the bourdon tube solved this problem; in fact this nut serves the dual purpose of anchoring the gauge in the mount and being removable

*In removing the filaments care must be exercised not to destroy the weave; otherwise it is very difficult to insert the damping material.

†The mount for the 20PAD-WS gauge was designed by D. G. Palmer of the Coyote Canyon Division of Sandia Corporation.

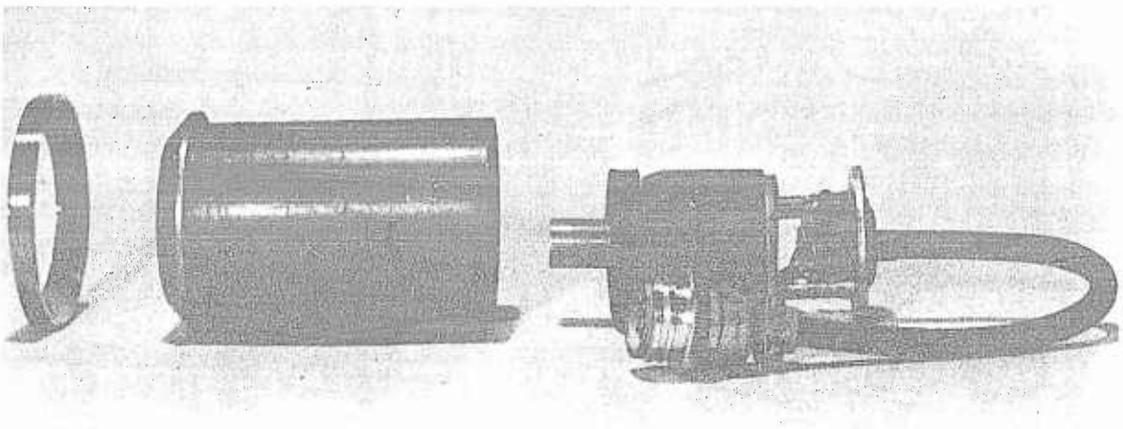

Fig. B.9 -- Semiexploded View of Canister for 3PAD Gauge, Showing Beveled End and Chamfered Retaining Ring

for attachment of the calibration fitting on the same set of threads. The low sensitivity of this gauge to acceleration made shock-mounting unnecessary, and it was feasible to affix the base of the gauge rigidly to a brass block which also formed a mounting for the cable connectors and decoupling resistors described in Appendix A. The complete mount for the 20PAD-WS gauge is installed in the pipe cap (Fig. B.11) in the same manner as the canister for the 3PAD gauge, using the chamfered retaining ring. This mount takes up considerably less space than the canister, and was designed to permit the opening of the sensing element to be flush with the surface across which pressures are to be measured without proximity to interfering obstructions. The spanner-wrench holes in the face are plugged with wax prior to taking pressure measurements.

Electrical connections to the 3PAD gauge were originally made through an AN connector affixed to the outer surface of the rear cover plate of the canister. It was found that by moving this connection farther out along the cable through a connector splice it was possible to achieve greater uniformity in the electrical system as well as economize on mounting space. Also the connectors are more accessible for repair. The same principle was applied in making connections to the 20PAD-WS gauge.

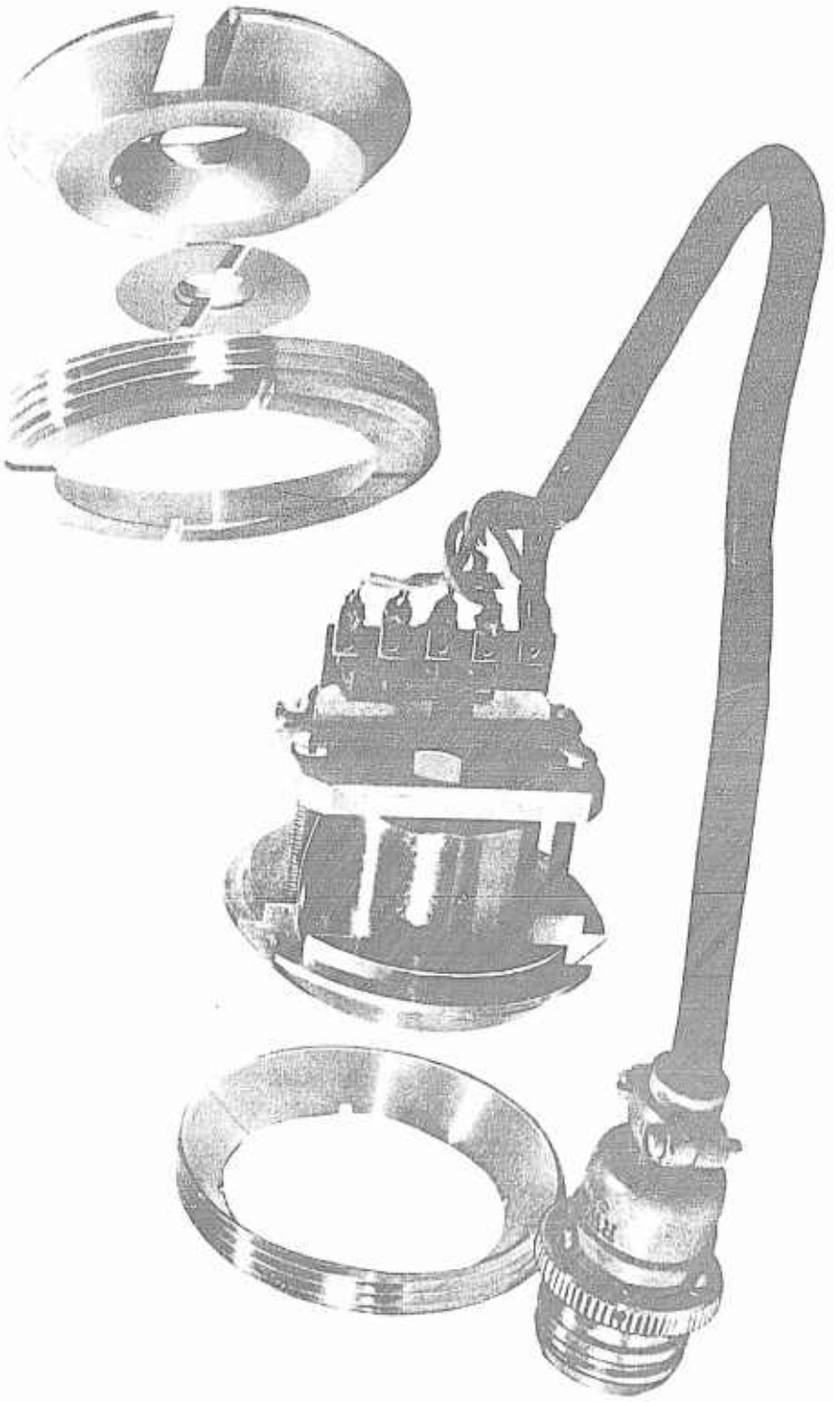

Fig. B.10 -- New Type Mount for the 20PAD-WS Gauge (Side View with Retaining Ring Removed). Inset shows front view of same mount (exploded).

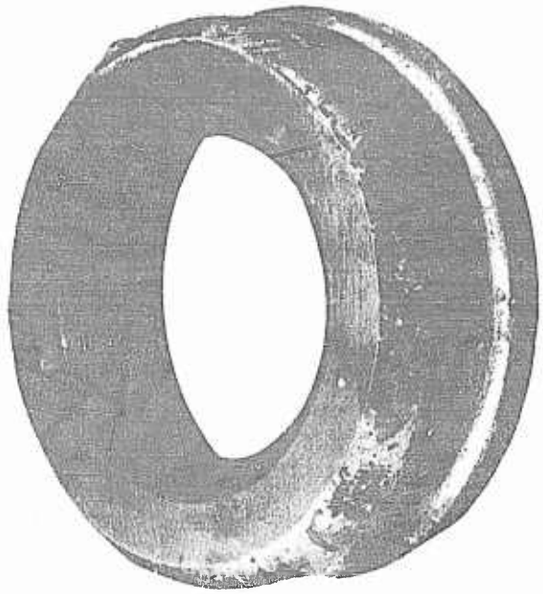

Fig. B.11 -- Pipe Cap Mount for Gauge

Moisture condensation on the terminals of the cables, the result of dropping temperatures, caused leakage between terminals that was great enough to create a sizeable and varying unbalance of the gauge system as sensed by the 20-kc carrier system (of Appendix A). Suitable coatings, such as Glyptal, were therefore applied to all terminals and exposed wires on the cables and on the gauges. Plastic sprays were experimented with for this purpose, but their tendency to peel allowed moisture to seep under the plastic film.

In designing the mounts for these gauges every effort was made to make the system as flexible as possible to incorporate continual changes and improvements.

DISTRIBUTION

Copy No.

ARMY ACTIVITIES

Asst. Chief of Staff, G-2, D/A, Washington 25, D. C.	1
Asst. Chief of Staff, G-3, D/A, Washington 25, D. C. ATTN: Dep. Asst. CofS, G-3, (RR&SW)	2
Asst. Chief of Staff, G-4, D/A, Washington 25, D. C.	3
Chief of Ordnance, D/A, Washington 25, D. C. ATTN: ORDTX-AR	4
Chief Signal Officer, D/A, P&O Division, Washington 25, D. C. ATTN: SIGOP	5- 7
The Surgeon General, D/A, Washington 25, D. C. ATTN: Chairman, Medical R&D Board	8
Chief Chemical Officer, D/A, Washington 25, D. C.	9- 10
Chief of Engineers, D/A, Military Construction Division, Protective Construction Branch, Washington 25, D. C. ATTN: ENGEB	11
Chief of Engineers, D/A, Civil Works Division, Washington 25, D. C. ATTN: Engineering Division, Structural Branch	12
The Quartermaster General, CBR, Liaison Office, Research and Development Division, D/A, Washington 25, D. C.	13
Office, Chief of Transportation, D/A, Washington 25, D. C. ATTN: Military Planning and Intelligence	14
Chief, Army Field Forces, Ft. Monroe, Va.	15- 17
Army Field Forces Board #1, Ft. Bragg, N. C.	18
Army Field Forces Board #2, Ft. Knox, Ky.	19
Army Field Forces Board #4, Ft. Bliss, Tex.	20
Commanding General, First Army, Governor's Island, New York 4, N. Y. ATTN: G-4, ACofS	21- 23
Commanding General, Second Army, Ft. George G. Meade, Md. ATTN: AIABB	24
Commanding General, Second Army, Ft. George G. Meade, Md. ATTN: AIAME	25
Commanding General, Second Army, Ft. George G. Meade, Md. ATTN: AIACM	26
Commanding General, Third Army, Ft. McPherson, Ga. ATTN: ACofS, G-3	27- 28
Commanding General, Fourth Army, Ft. Sam Houston, Tex. ATTN: G-3 Section	29- 30
Commanding General, Fifth Army, 1660 Hyde Park Blvd., Chicago 15, Ill. ATTN: ALFEN	31
Commanding General, Fifth Army, 1660 Hyde Park Blvd., Chicago 15, Ill. ATTN: ALFOR	32
Surplus in TISOR	33- 36

DISTRIBUTION (Continued)

	Copy No.
Commanding General, Sixth Army, Presidio of San Francisco, Calif. ATTN: AMGCT-4	37
Commander-in-Chief, European Command, APO 403, c/o PM, New York, N. Y.	38
Commander-in-Chief, U. S. Army Europe, APO 403, c/o PM, New York, N. Y. ATTN: OPOT Division, Com. Dev. Branch	39- 40
Commander-in-Chief, Far East Command, APO 500, c/o PM, San Francisco, Calif. ATTN: ACofS, J-3	41- 42
Commanding General, U. S. Army Forces Far East (Main), APO 343, c/o PM, San Francisco, Calif. ATTN: ACofS G-3	43- 45
Commanding General, U. S. Army Alaska, APO 942, c/o PM, Seattle, Wash.	46
Commanding General, U. S. Army Caribbean, APO 834, c/o PM, New Orleans, La. ATTN: CG, USARCARIB	47
Commanding General, U. S. Army Caribbean, APO 834, c/o PM, New Orleans, La. ATTN: CG, USARFANT	48
Commanding General, U. S. Army Caribbean, APO 834, c/o PM, New Orleans, La. ATTN: Cml. Off., USARCARIB	49
Commanding General, U. S. Army Caribbean, APO 834, c/o PM, New Orleans, La. ATTN: Surgeon, USARCARIB	50
Commanding General, USAR Pacific, APO 958, c/o PM, San Francisco, Calif. ATTN: Cml. Off.	51- 52
Commanding General, Trieste U. S. Troops, APO 209, c/o PM, New York, N. Y. ATTN: ACofS, G-3	53
Commandant, Command and General Staff College, Ft. Leavenworth, Kan. ATTN: ALLIS(AS)	54- 55
Commandant, The Infantry School, Ft. Benning, Ga. ATTN: C.D.S.	56- 57
Commandant, The Artillery School, Ft. Sill, Okla.	58
Commandant, The AA&GM Branch, The Artillery School, Ft. Bliss, Tex.	59
Commandant, The Armored School, Ft. Knox, Ky. ATTN: Classified Document Section, Evaluation and Res. Division	60- 61
Commanding General, Medical Field Service School, Brooke Army Medical Center, Ft. Sam Houston, Tex.	62
Commandant, Army Medical Service School, Walter Reed Army Medical Center, Washington 25, D. C. ATTN: Dept. of Biophysics	63
The Superintendent, United States Military Academy, West Point, N. Y. ATTN: Professor of Ordnance	64- 65
Commanding General, The Transportation Corps Center and Ft. Eustis, Ft. Eustis, Va. ATTN: Asst. Commandant, Military Sciences and Tactics	66
Commandant, Chemical Corps School, Chemical Corps Training Command, Ft. McClellan, Ala.	67
Commanding General, Research and Engineering Command, Army Chemical Center, Md. ATTN: Special Projects Officer	68

DISTRIBUTION (Continued) — Copy No.

RD Control Officer, Aberdeen Proving Ground, Md. ATTN: Director, Ballistics Research Laboratory	69- 70
Commanding General, The Engineer Center, Ft. Belvoir, Va. ATTN: Asst. Commandant, The Engineer School	71- 73
Chief of Research and Development, D/A, Washington 25, D. C.	74
Commanding Officer, Engineer Research and Development Laboratory, Ft. Belvoir, Va. ATTN: Chief, Technical Intelligence Branch	75
Commanding Officer, Picatinny Arsenal, Dover, N. J. ATTN: ORDBB-TK	76
Commanding Officer, Army Medical Research Laboratory, Ft. Knox, Ky.	77
Commanding Officer, Chemical Corps Chemical and Radiological Laboratory, Army Chemical Center, Md. ATTN: Technical Library	78- 79
Commanding Officer, Transportation R&D Station, Ft. Eustis, Va.	80
Commanding Officer, Psychological Warfare Center, Ft. Bragg, N. C. ATTN: Library	81
Asst. Chief, Military Plans Division, Rm 516, Bldg. 7, Army Map Services, 6500 Brooks Lane, Washington 25, D. C. ATTN: Operations Plans Branch	82
Director, Technical Documents Center, Evans Signal Laboratory, Belmar, N. J.	83
Director, Waterways Experiment Station, PO Box 631, Vicksburg, Miss. ATTN: Library	84
Director, Operations Research Office, Johns Hopkins University, 6410 Connecticut Ave., Chevy Chase, Md. ATTN: Library	85

NAVY ACTIVITIES

Chief of Naval Operations, D/N, Washington 25, D. C. ATTN: OP-36	86- 87
Chief of Naval Operations, D/N, Washington 25, D. C. ATTN: OP-51	88
Surplus in TISOR	89
Chief of Naval Operations, D/N, Washington 25, D. C. ATTN: OP-374 (OEG)	90
Chief, Bureau of Medicine and Surgery, D/N, Washington 25, D. C. ATTN: Special Weapons Defense Division	91- 92
Chief, Bureau of Ordnance, D/N, Washington 25, D. C.	93
Chief, Bureau of Personnel, D/N, Washington 25, D. C. ATTN: Pers 15	94
Chief, Bureau of Personnel, D/N, Washington 25, D. C. ATTN: Pers C	95
Chief, Bureau of Ships, D/N, Washington 25, D. C. ATTN: Code 348	96

DISTRIBUTION (Continued)

	Copy No.
Chief, Bureau of Supplies and Accounts, D/N, Washington 25, D. C.	97
Chief, Bureau of Yards and Docks, D/N, Washington 25, D. C. ATTN: P-312	98
Chief, Bureau of Aeronautics, D/N, Washington 25, D. C.	99-100
Office of Naval Research, Code 219, Rm 1807, Bldg. T-3, Washington 25, D. C. ATTN: RD Control Officer	101
Commander-in-Chief, U. S. Atlantic Fleet, Fleet Post Office, New York, N. Y.	102-103
Commander-in-Chief, U. S. Pacific Fleet, Fleet Post Office, San Francisco, Calif.	104-105
Commander, Operation Development Force, U. S. Atlantic Fleet, U. S. Naval Base, Norfolk 11, Va. ATTN: Tactical Development Group	106
Commander, Operation Development Force, U. S. Atlantic Fleet, U. S. Naval Base, Norfolk 11, Va. ATTN: Air Department	107
Commandant, U. S. Marine Corps, Headquarters, USMC, Washington 25, D. C. ATTN: (A03H)	108-111
President, U. S. Naval War College, Newport, Rhode Island	112
Superintendent, U. S. Naval Postgraduate School, Monterey, Calif.	113
Commanding Officer, U. S. Naval Schools Command, Naval Station, Treasure Island, San Francisco, Calif.	114-115
Director, USMC Development Center, USMC Schools, Quantico, Va. ATTN: Marine Corps Tactics Board	116
Director, USMC Development Center, USMC Schools, Quantico, Va. ATTN: Marine Corps Equipment Board	117
Commanding Officer, Fleet Training Center, Naval Base, Norfolk 11, Va. ATTN: Special Weapons School	118-119
Commanding Officer, Fleet Training Center, (SPWP School), Naval Station, San Diego 36, Calif.	120-121
Commander, Air Force, U. S. Pacific Fleet, Naval Air Station, San Diego, Calif.	122
Commander, Training Command, U. S. Pacific Fleet, c/o Fleet Sonar School, San Diego 47, Calif.	123
Commanding Officer, Air Development Squadron 5, USN Air Station, Moffett Field, Calif.	124
Commanding Officer, Naval Damage Control Training Center, U. S. Naval Base, Philadelphia 12, Pa. ATTN: ABC Defense Course	125
Commanding Officer, Naval Unit, Chemical Corps School, Ft. McClellan, Ala.	126
Joint Landing Force Board, Marine Barracks, Camp Lejeune, N. C.	127

DISTRIBUTION (Continued) Copy No.

Commander, U. S. Naval Ordnance Laboratory, Silver Spring 19, Md. ATTN: EE	128
Commander, U. S. Naval Ordnance Laboratory, Silver Spring 19, Md. ATTN: Alias	129
Commander, U. S. Naval Ordnance Laboratory, Silver Spring 19, Md. ATTN: Aliex	130
Commander, U. S. Naval Ordnance Test Station, Inyokern, China Lake, Calif.	131
Officer-in-Charge, U. S. Naval Civil Engineering Research and Evaluation Laboratory, Construction Battalion Center, Port Hueneme, Calif. ATTN: Code 753	132-133
Commanding Officer, USN Medical Research Institute, National Naval Medical Center, Bethesda 14, Md.	134
Director, U. S. Naval Research Laboratory, Washington 25, D. C.	135
Commanding Officer and Director, USN Electronics Laboratory, San Diego 52, Calif. ATTN: Code 210	136
Commanding Officer, USN Radiological Defense Laboratory, San Francisco, Calif. ATTN: Technical Information Division	137-138
Commanding Officer and Director, David W. Taylor Model Basin, Washington 7, D. C. ATTN: Library	139
Commander, Naval Air Development Center, Johnsville, Pa.	140
Commanding Officer, Office of Naval Research Branch Office, 1000 Geary St., San Francisco, Calif.	141-142

AIR FORCE ACTIVITIES

Surplus in TISOR	143
Asst. for Atomic Energy, Headquarters, USAF, Washington 25, D. C. ATTN: DCS/O	144
Asst. for Development Planning, Headquarters, USAF, Washington 25, D. C.	145-146
Director of Operations, Headquarters, USAF, Washington 25, D. C.	147-148
Director of Plans, Headquarters, USAF, Washington 25, D. C. ATTN: War Plans Division	149
Directorate of Requirements, Headquarters, USAF, Washington 25, D. C. ATTN: AFDRQ-SA/M	150
Directorate of Research and Development, Armament Division, DCS/D, Headquarters, USAF, Washington 25, D. C.	151
Directorate of Intelligence, Headquarters, USAF, Washington 25, D. C.	152-153
The Surgeon General, Headquarters, USAF, Washington 25, D. C.	154-155
Commanding General, U. S. Air Forces Europe, APO 633, c/o PM, New York, N. Y.	156

DISTRIBUTION (Continued)

	Copy No.
Commanding General, Far East Air Forces, APO 925, c/o PM, San Francisco, Calif.	157
Commanding General, Alaskan Air Command, APO 942, c/o PM, Seattle, Wash. ATTN: AAOTN	158-159
Commanding General, Northeast Air Command, APO 862, c/o PM, New York, N. Y.	160
Commanding General, Strategic Air Command, Offutt AFB, Omaha, Neb. ATTN: Chief, Operations Analysis	161
Commanding General, Tactical Air Command, Langley AFB, Va. ATTN: Documents Security Branch	162-164
Commanding General, Air Defense Command, Ent AFB, Colo.	165-166
Commanding General, Air Materiel Command, Wright-Patterson AFB, Dayton, Ohio	167-169
Commanding General, Air Training Command, Scott AFB, Belleville, Ill.	170-171
Commanding General, Air Research and Development Command, PO Box 1395, Baltimore 3, Md. ATTN: RDDN	172-174
Commanding General, Air Proving Ground Command, Eglin AFB, Fla., ATTN: AG/TRB	175
Commanding General, Air University, Maxwell AFB, Ala.	176-177
Surplus in TISOR	178-180
Commandant, Air Command and Staff School, Maxwell AFB, Ala.	181-182
Commandant, Air Force School of Aviation Medicine, Randolph AFB, Tex.	183-184
Commanding General, Wright Air Development Center, Wright-Patterson AFB, Dayton, Ohio. ATTN: WCOESP	185-190
Commanding General, Air Force Cambridge Research Center, 230 Albany St., Cambridge 39, Mass. ATTN: Atomic Warfare Directorate	191
Commanding General, Air Force Cambridge Research Center, 230 Albany St., Cambridge 39, Mass. ATTN: CRTSL-2	192
Commanding General, AF Special Weapons Center, Kirtland AFB, N. Mex. ATTN: Chief, Technical Library Branch	193-195
Commandant, USAF Institute of Technology, Wright-Patterson AFB, Dayton, Ohio. ATTN: Resident College	196
Commanding General, Lowry AFB, Denver, Colo. ATTN: Dept. of Armament Training	197-198
Commanding General, 1009th Special Weapons Squadron, Tempo "T", 14th & Constitution Sts., N.W., Washington, D. C.	199-201
The RAND Corporation, 1700 Main St., Santa Monica, Calif. ATTN: Nuclear Energy Division	202-203

OTHER DEPT. OF DEFENSE ACTIVITIES

Executive Secretary, Joint Chiefs of Staff, Washington 25, D. C.	204

DISTRIBUTION (Continued)

	Copy No.
Director, Weapons Systems Evaluation Group, OSD, Rm 2E1006, Pentagon, Washington 25, D. C.	205
Asst. for Civil Defense, OSD, Washington 25, D. C.	206
Chairman, Armed Services Explosives Safety Board, D/D, Rm 2403, Barton Hall, Washington 25, D. C.	207
Chairman, Research and Development Board, D/D, Washington 25, D. C. ATTN: Technical Library	208
Executive Secretary, Committee on Atomic Energy, Research and Development Board, Rm 3E1075, Pentagon, Washington 25, D. C.	209-210
Executive Secretary, Military Liaison Committee, PO Box 1814, Washington 25, D. C.	211
Commandant, National War College, Washington 25, D. C. ATTN: Classified Records Section, Library	212
Commandant, Armed Forces Staff College, Norfolk 11, Va. ATTN: Secretary	213
Commanding General, Field Command, AFSWP, PO Box 5100, Albuquerque, N. Mex.	214-219
Chief, AFSWP, PO Box 2610, Washington 13, D. C.	220-228

ATOMIC ENERGY COMMISSION ACTIVITIES

University of California Radiation Laboratory, PO Box 808, Livermore, Calif. ATTN: Margaret Folden	229
U. S. Atomic Energy Commission, Classified Document Room, 1901 Constitution Ave., Washington 25, D. C. ATTN: Mrs. J. M. O'Leary (for DMA)	230-232
Los Alamos Scientific Laboratory, Report Library, PO Box 1663, Los Alamos, N. Mex. ATTN: Helen Redman	233-235
Sandia Corporation, Classified Document Division, Sandia Base, Albuquerque, N. Mex. ATTN: Wynne K. Cox	236-255
Special Projects Branch, TISOR	256
Surplus in TISOR for AFSWP	257-281

ADDITIONAL DISTRIBUTION

Director of Special Weapons Developments, OCAFF, Fort Bliss, Texas. ATTN: Major Hale Mason, Jr.	282
Director of Operations, Hqs., USAF, Washington 25, D.C. ATTN: Operations Analysis Division	283